VILNIUS UNIVERSITY

VILNIUS PEDAGOGICAL UNIVERSITY

Marius Franckevičius

EXCITED-STATE DYNAMICS OF PPI AND PAMAM DENDRIMERS FUNCTIONALIZED WITH PHOTOCHROMIC TERMINAL GROUPS

Doctoral thesis
Physical sciences, physics (02 P)

Vilnius, 2011

The thesis was prepared at Vilnius pedagogical university, in Liquid crystals laboratory in 2007-2011.

Scientific supervisor:

prof. habil. dr. Donatas Rimantas Vaišnoras (Vilnius pedagogical university, Physical sciences, physics – 02 P)

Scientific advisor:

prof. habil. dr. Vidmantas Gulbinas (Center for physical sciences and technology / Institute of physics, Physical sciences, physics – 02 P)

Content

Introduction

Dendrimers are multivalent, well-defined materials that constitute a new class of polymer macromolecules. They have been extensively studied over the past several decades, mainly due to their exceptional structure properties. The size of molecule, number of terminal groups, molecular weight and several other properties of dendrimers could be precisely controlled during synthesis. Moreover, their randomly hyperbranched functionalities with chemically reactive terminal groups are ideal places where various chemical compounds could be attached [1]. Depending on the type of function groups, various physical, chemical or biological properties of these molecules could be controlled. Relatively simple chemical modification of dendrimers already allows to use them for development of drug delivery systems, substances suitable mimicking biological systems and other new materials attractive from both scientific and technological perspectives [1].

Because many properties of dendrimers could be tuned depending on the type of their functional groups, those concerning the controlled response to light have large potential applications [2]. The interraction of light can cause large change in the conformation of organic photochromic materials and thus has profound influence on their physical and chemical properties. Changes associated with *trans-cis* isomerization of azobenzenes, can be used to rearrange wide variety of organized media. At the same time materials with light induced proton transfer ability are of special interest in many of biological applications. In order to improve photochromical behaviour and at the same to extend their application perspectives most of photochromic materials have been chemically incorporated within different matrices including: polymers, liquid crystals or dendrimers [3, 4, 5, 6]. Simultaneously, dendrimers as a new distinguished class of superbranched molecules hold a special place among a large number of photochromic compounds. It results an interesting environment to explore the molecular movements and photochemical reactions affected by cage effect and mimic the

environments in the large molecules such as proteins, polymers and other supramolecular systems [7, 8].

In the this thesis, we concentrate on the relaxation dynamics of the newly synthesized PPI and PAMAM dendrimers terminated with two types of photochromic compounds. First one belongs to the azobenzene type photochromes and a second one to the Schiff base containing materials. Various photophysical processes may be challenged within those systems during the interaction with light. Among them, light induced *trans-cis* isomerization and enol-keto tautomerization reactions are of great importance.

Main goal and objectives

The **goal** of this thesis is to investigate optical properties and light induced photochemical reaction dynamics within PPI and PAMAM dendrimers functionalized with cyanoazobenzene (CAzPA) and 4-(4'-ethoxybenzoyloxy)salicylaldehyde (ESA) type terminal groups, by means of steady state absorption, fluorescence and time resolved transient absorption spectroscopy.

Tasks:

- To evaluate factors affecting morphology of PPI dendrimer solid films.
- To determine the near UV absorption properties of pure amine-terminated PPI dendrimer within dimethylsulfoxide solution.
- To investigate spectroscopic and dynamics properties of PPI and PAMAM dendrimers functionalized CAzPA type terminal groups.
- To identify formation of possible tautomeric forms within the PPI dendrimers functionalized ESA type terminal groups and to reveal their spectroscopic and dynamics properties.

Novelty and importance

In this dissertation original results based on the investigations of optical and excited state dynamics properties of the dendrimers functionalized with

photochromic CAzPA and ESA type molecules as terminal groups are presented for the firs time. The obtained results provide better understanding about the dynamics behavior within the dendrimer functional groups depending on the dendrimer type and its generation. Since there is possibility to the fast and efficient control of the functional groups, dendrimer could be used for various applications.

The points to be maintained

- Isomerization of PPI and PAMAM dendrimers functionalized with CAzPA type photochromical terminal groups takes place independently of the dendrimer type, excitation wavelength and solvent. The isomerization rate in solutions and in solid films is determined mainly by the flexibility of the chromophore groups and their interactions with other dendrimer parts as than interaction with the dendrimer environment.
- Domination of the tautomeric forms within the ESA type chromophore groups of PPI dendrimer depends on its generation, and their fluorescence yield and excited state dynamics depend on the excitation wavelength. Hydrogen bonds between chromophore groups determine their tautomerism and their dynamical properties.
- Light induced conformational changes of CAzPA and ESA functional groups of dendrimers provide opportunities to control optical and structural changes of dendrimers.

Layout of the thesis

The thesis consists of introduction, six chapters, main conclusions and list of references:

Chapter 1. The first section of this chapter provides an overview of the dendrimers as a new class of polymeric macromolecules. Here a brief discussion about their synthesis, structure, properties and functionalization

perspectives is presented. In the second half of this chapter, more attention is paid to the analysis of photochromical materials and photochemical reactions. Photoisomerization and phototautomerization within the azobenzene and Schiff base containing materials will be also discussed in more detail.

The ***Chapter 2*** describes basic properties of each investigated dendrimer including their structure and brief introduction to the synthesis. Experimental techniques used for the dendrimer characterization are also described in this chapter.

The following four chapters the main results are described.

The first section of the ***Chapter 3*** is devoted to the study of the surface morphology of PPI dendrimer films deposited from different solvents on different surfaces. Atomic force microscopy (AFM) is used to imagine the morphology of the thin films. Whereas in the next section, the optical properties of amine-terminated PPI dendrimers in dichloromethane solution are presented.

Excited state relaxation of PPI and PAMAM dendrimers functionalized with CAzPA type terminal groups are presented in ***Chapter 4***. Steady-state spectroscopy provides detailed information about the optical properties of both dendrimers. Wheres relaxation dynamics within the materials were determined by using transient absorption investigations.

In ***Chapter 5*** the results of exciton relaxation and migration in the PPI-ESA dendrimer solvents and films are presented. The importance of interchromophore interactions on exciton migration within the dendrimer solids are discussed in more detail.

The last ***Chapter 6*** deals with the tautmeric behaviour of the first and fifth generation PPI dendrimers, functionalized with ESA type terminal groups. Influence on UV absorption and fluorescence properties of ESA photochromic groups are discussed. Excited state dynamics behavior of intramolecular proton transfer is discussed as well.

The author's contribution

Most of the obtained experimental results presented within the thesis have been carried out by the author under the guidance by prof. R. Vaišnoras[1] and prof. V. Gulbinas[2].

Structural studies of dendrimers performed by AFM were carried out in contributions with prof. J. Babonas[3] and prof. I. Šimkienė[3], as well as with dr. Amir Fahmi[4].

Fluorescence kinetics measurements by streak camera were performed under the coordination of prof. C. Lopez[5].

Author has also contributed in the preparation of the articles and conference abstracts.

Joint authors have performed other works related with the thesis.. Prof. J.L. Serrano[6] and M. Marcos[6] have synthesized dendrimers.

A. Gruodis[7] and J. Tamulienė[8] have performed quantum chemical calculations. .

[1] Liquid Crystals Laboratory, Faculty of Physics and Technology, Vilnius Pedagogical University, Vilnius, Lithuania.

[2] Center for Physical Sciences and Technology, Institute of Physics, Vilnius, Lithuania.

[3] Semiconductor Physics Institute of the Center for Physical Sciences and Technology, Vilnius, Lithuania.

[4] Department of Mechanical, Materials and Manufacturing Engineering, University of Nottingham, Nottingham, United Kingdom.

[5] Instituto de Ciencia de Materiales de Madrid (ICMM), Madrid, Spain.

[6] Instituto de Ciencia de Materiales de Aragon (ICMA), Universidad de Zaragoza, Saragosa, Spain.

[7] Faculty of physics, Vilnius University, Vilnius, Lithuania.

[8] Institute of Theorethical Physics and Astronomy of Vilnius University, Vilnius, Lithuania.

Acknowledgements

I first wish to thank my supervisor prof. Rimantas Vaišnoras for great confidence, inexhaustible ideas and given opportunity to work in the field of science. I thank all of my colleagues dr. Loreta Rasteniene and Augustinas Kulbickas.

I would also like to thank whole Experimental nanophysics group of Institute of Physics of the Center for Physical Sciences and Technology. Particularly thanks to my scientific supervisor prof. Vidmantas Gulbinas and also to dr. Renata Karpicz for disscusions, their help during experiments and preparation of articles.

I'm also thankful to whole faculty of physics and technology of Vilnius pedagogical university and especially to department of physics and information technologies.

I also thank to prof. Jurgis Gintautas Babonas, dr. Alfonsas Rėza, and prof. Irena Šimkienė for their help during the structural investigations of dendrimers, consultations and discussions.

I acknowledge joint authors and other colleagues working abroad prof. Jose Luis Serrano, dr. Mercedes Marcos, prof. Cefe Lopez, dr. Martin Lopez Garcia, dr. Amir Fahmi, Nicol Cheval and Vladimir Astachov.

Thanks to all my friends.

Most of all, I would like to thank my Mother and girlfriend Aistė for their strong support during all these years.

This work has been supported by projects: COST TD0802 and PHOREMOST (N511616). Also thanks to the Lithuanian State Science and Studies Fundation.

Approbation

List of publications related to the thesis:

[P.1] **M. Franckevičius**, M. Marcos, J.L. Serrano, R. Karpicz, V. Gulbinas, and R. Vaišnoras, Excited-state relaxation of dendrimers functionalized with cyanoazobenzene-type terminal groups, *Chemical Physics Letters*, **485**, 156 (2010).

[P.2] J. Tamulienė, **M. Franckevičius,** L. Rastenienė, A. Kulbickas, R. Vaišnoras, and G. Badenes, Structure modeling of Co-encapsulated PPI dendrimer*, Journal of Nanoscience and Nanotechnology*, **10**, 6407 (2010).

[P.3] I. Minevičiūtė, V. Gulbinas, **M. Franckevičius**, R. Vaišnoras, M. Marcos, and J.L. Serrano, Exciton Migration and Quenching in poly(propylene-imine) dendrimers, *Chemical Physics,* **359**, 65 (2009).

[P.4] **M. Franckevicius**, PPI dendrimers encapsulated with silver nanoparticles as carriers for medical applications, *Poceedings of the 7th international conference on medical physics*, **7**, 34 (2009).

[P.5] A. Kulbickas, J. Tamuliene, L. Rasteniene, **M. Franckevicius**, R. Vaisnoras, M. Marcos, J.L. Serrano, B. Jaskorzynska, and L. Wosinski, Optical study and structure modelling of PPI liquid crystalline dendrimer derivatives, *Photonics and Nanostructures - Fundamentals and Applications*, **5**, 178 (2007).

[P.6] **M. Franckevičius**, Nematinių skystakristalinių dendrimerų optinių savybių tyrimai, Lietuvos jaunųjų mokslininku konferencijos "Mokslas - Lietuvos ateitis" medžiaga, Vilnius: Technika, 170 (2008).

[P.7] **M. Franckevičius**, J. Tamulienė, J. Babonas, L. Rastenienė, A. Kulbickas, I. Šimkiene, I. Iržikevičius, and R. Vaišnoras, UV Spectral Features of Poly(propylene imine) Dendrimers, *Lithuanian Journal of Physics*, (2011). (accepted).

[P.8] **M. Franckevičius**, R. Vaišnoras, A. Gruodis, N. Galikova, M. Marcos, J.L. Serrano, and V. Gulbinas, Tautomeric forms and excited state dynamics of PPI dendrimers functionalized with ESA chromophores, *J. Phys. Chem. A*, (2011). (submitted).

Other publications:

[P.9] I. Šimkiene, A. Reza, A. Kindurys, V. Bukauskas, J. Babonas, R. Szymczak, P. Aleshkevych, **M. Franckevicius**, and R. Vaišnoras, Magnetooptics of opal crystals modified by cobalt nanoparticles, *Lithuanian Journal of Physics*, **50**, 7 (2010).

List of conferences contributions related to the thesis:

[C.1] M. Franckevičius. *Dendrimers as drug nanocontainers*. "Medical Physics 2009". October 08-10, 2009, Kaunas, Lithuania.

[C.2] R. Karpicz, V. Gulbinas, M. Franckevičius, and R. Vaišnoras. *Exiton migration and relaxation in PPI and PAMAM dendrimers*. XIX International School-Seminar "Spectroscopy of Molecules and Crystals". September 20-27, 2009, Beregove, Crimea, Ukraine.

[C.3] M. Franckevičius, R. Vaišnoras, M. Marcos, J.L. Serrano, R. Karpicz, and V. Gulbinas. *Excited state relaxation of dendrimers functionalized with cyanoazobenzene-type terminal groups*. XVIII Lithuanian-Belarus Seminar, September, 16-18, 2009, Vilnius, Lithuania.

[C.4] M. Franckevičius, J. Tamulienė, M. Marcos, J.L. Serrano, J. Babonas, I. Šimkiene, and R. Vaišnoras, *Structure modeling of Co-encapsulated PPI dendrimers.* Lithuanian National Physics Conference, May 8-10, 2009, Vilnius, Lithuania.

[C.5] L. Rastenienė, A. Kulbickas, M. Franckevičius, J. Tamulienė, R. Vaišnoras, M. Marcos, J.L. Serrano, J. Babonas, I. Šimkiene, and C. Lopez. *Optical spectra of functionalized liquid crystalline poly(propylene-imine) dendrimers*. International school on nanophotonics and molecular photonics. June 16-20, 2008, Santander, Spain.

[C.6] L. Rastenienė, A. Kulbickas, M. Franckevičius, R. Vaisnoras, M. Marcos, J.L. Serrano, J. Babonas, I. Šimkienė, and C. Lopez. *Optical spectra of functionalized liquid crystalline poly(propylene-imine) dendrimers*. EMRS. May 26-30, 2008, Strasbourg, France.

[C.7] M. Franckevičius. *Nematinių skystakristalinių dendrimerų optinių savybių tyrimai*. 11-oji Lietuvos jaunųjų mokslininkų konferencija. April 4, 2008, Vilnius, Lithuania.

[C.8] I. Minevičiūtė, R. Vaišnoras, M. Franckevičius, and V. Gulbinas. Exciton migration in poly(propylene-imine) dendrimers. The 6th International Conference "Advanced Optical Materials and Devices". August 24-27, 2008, Riga, Latvia.

List of Abbreviations

AFM	Atomic force microscopy
CAzPA	Cyanoazobenzene
CCD	Charge coupled device
CHF	Chloroform
DAB	Diaminobutane
DMSO	Dimethyl sulfoxide
DCM	Dichloromethane
EDA	Ethylenediamine
ESA	4-(4'-ethoxybenzoyloxy)salicylaldehyde
ESIPT	Excited state intramolecular proton transfer
GSIPT	Ground state intramolecular proton transfer
Nd:YAG	Neodymium doped yttrium aluminum garnet
OD	Optical density
PAMAM	Poly(amidoamine)
PPI	Poly(propylene-imine)
SA	Salicylidene-aniline
SEM	Scanning electron microscopy
TA	Transient absorption
TEM	Transmission electron microscopy
THF	Tetrahydrofuran

1. Literature analysis

Polymers are large molecules composed of numerous monomers covalently connected to each other. These large compounds are divided into the two broad groups: synthetic and biological polymers. Synthetic polymers are man-made macromolecules while biological polymers have dual nature, they could be both synthetic and natural, for instance, peptide. The idea that bio-polymers and man-made polymers are composed of a very large molecules, named *macromolecules*, was invented and adapted by Herman Staudinger in 1930 [9]. This led to the evolution of the three major macromolecular architectures: linear, cross-linked and branched. They are often referred to as synthetic polymers and have been well studied in the past [10].

Formation concepts of the new class polymer macromolecules composed of various complexity molecular species was reported by Paul Flory in a series of his early works as far back as 1941 [11]. However, Fritz Vögtle first introduced the synthesis of low molecular weight cascade molecules only after several decades in 1978 [12]. Whereas Donald Tomalia using the method developed by Vögtle has synthesized the three-dimensional repetitively branched molecules for the first time in 1985 [13]. These newly-designed compounds received a new term, recently known as dendrimers. A term is derived from the Ancient Greek words, *dendron* (*gr*. δενδρον), meaning tree, and *meros* (*gr.* μεροσ), meaning to part. According to Tomalia, dendritic topology has now been recognized as a fourth major class of molecular architecture in the polymer field [14]. Dendrimers together with randomly hyperbranched polymers [15], dendrigraft polymers [16] and dendronized polymers [17] are attributed to this new class of polymeric macromolecules.

After these pioneering discoveries, rapid growth in the study of dendrimers expands to the different areas including theory, synthesis, characterization of structure, investigation of potential applications and many others [18, 19].

1.1. A brief introduction to dendrimers

1.1.1. Synthesis of dendrimers

There are two main methods generally used for synthesis of dendrimer. The first one is divergent, introduced by Tomalia [13] and Newcome [20] in the middle of 80's and a second one – convergent approach, developed by Hawker and Fréchet in the 1990 [21]. Both synthesis techniques are schematically shown in Fig. 1.1. As can be seen, the dendrimer growth direction is the most obvious difference between these two approaches. In the divergent method (approach) the synthesis starts at the central multifunctional core and radially extends into the surface, whereas in convergent method *vice versa*. Relatively high-generation macromolecules (it depends on the chemical composition of structural elements) could be synthesized by using divergent

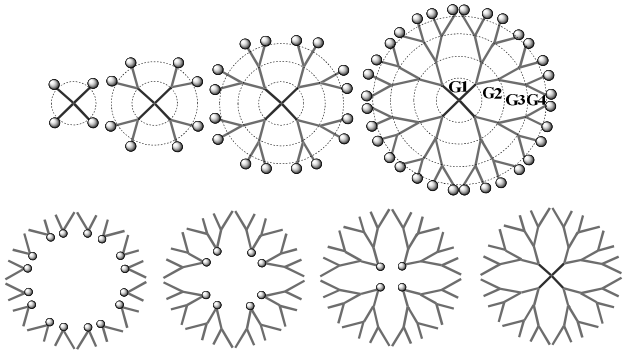

Fig. 1.1. The schemes representing two different dendrimer synthesis methods (from left to right). The top figures show divergent approach and below – convergent. The circles mark functionalizing units.

synthesis approach. However, the main disadvantage of this method is concerned with the amount of structural defects, which begin to emerge at higher generations when a large number of coupling or condensation reactions have to occur on the congested dendrimer surface [22]. It can thus be considered that divergent method can lead to a decrease in the quality of dendrimer as its generation increases [23]. Despite of this, majority of dendrimer types have been synthesized divergently until now. Poly(propylene-

imine) (PPI) and poly(amidoamine) (PAMAM) are the best examples of all of them.

The second conceptually different method for the dendrimer synthesis follows a convergent growth process. Using this method, macromolecule is constructed from the periphery to the center when two or more dendrons are coupled with each other at the core unit. It is often argue that latter method was developed as a response to all weaknesses emerging in the divergent synthesis. The most obvious advantage of convergent approach is concerned with the low amount of defects which number can be thereby reduced during the purification process. However, high-quality dendrimers can be achieved at the expense of their low generations. Formation of the higher generations is restricted, because steric problems begin to occur in the reactions between the dendrons and the core molecule [24]. In addition, convergent approach is commonly used in order to create multifunctional dendrimers. They are made up of dendrons of different types that are coupled together with multifunctional core [25]. Despite all mentioned differences, both methods are complementary and widely used for the synthesis of different dendrimer types [26].

Physical properties (size, shape, molecular weight) as well as chemical properties (solubility, viscosity, polydispersity and *etc.*) of most dendrimers could be effectively controlled during the synthesis by appropriate selection of core, monomers and functional groups [23, 26]. Since their discovery, more than 25 years ago, hundreds of compositionally different dendrimer families have been synthesized [27]. Such a large number of different dendrimers is directly related with the immense quantities of materials that can be selected for their synthesis. For example, Ponomarenko et al. have shown possibility to design huge amount of liquid crystalline dendrimers possessing compositionally different building blocks [28]. But despite giving a far more detailed description of a specific type of dendrimer, let us briefly describe the typical structural properties of almost all of dendrimer types in the next section.

1.1.2. Structure of dendrimers

Dendrimers being intermediate between polymers and low molecular mass compounds are described as a new class of synthetic macromolecules. They possess well-defined, highly branched and perfectly monodispersed architectures. The structure of dendrimer macromolecule consist of the three major topologically different architectural building blocks: central core, internal branching units and terminal end groups. A typical example of the dendrimer structure is presented in Fig. 1.2.

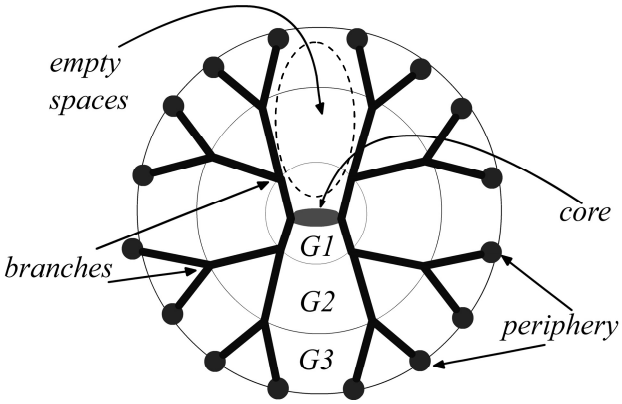

Fig. 1.2. Schematic representation of the typical dendrimer structure.

Multi-functional ***core*** located in the central part of the dendrimer macromolecule constitute a single atom or an atom group with at least two chemically active sites where different monomers could be added (typically obtained core functionalities are in the range between $2 \le f_m \le 8$). A wide range of chemical compounds can be successfully incorporated into the centre of dendrimer. The most commonly used molecules are organic by nature, but it is not prerequisite, because under certain circumstances different inorganic, ionic or organo-metallic composites as the central part of dendrimer macromolecule could be used as well [29-31]. Because core unit has a decisive influence on the size, shape, directionality and multiplicity of dendrimer [32], these functions could be easily tuned by selective choice of the core material.

The ***branches*** emanating from the central part of the dendrimer are identified as internal branching units. They consist of individual monomers usually with more than one functional group. Linked to each other they initiate formation of additional generations and gradually increase size of the dendrimer. Monomers suitable for preparation of dendrimer are usually composed of synthetic molecules with alkyl or aromatic moieties. In some cases, various molecules, such as carbohydrates, amino acids, nucleotides or dyes could be applied as monomers as well [33, 34].

Topologically dendritic polymer is composed of a sequence of concentric layers surrounding the core molecule. These layers defined as dendrimer generations (G*n*, where *n* is generation number) (see Fig. 1.1 and Fig. 1.2) are frequently used to determine the size of macromolecule within a given dendrimer type. The total number of monomers *N* within the dendrimer of a certain generation can be obtained from the following equation [35]:

$$N = 1 + f_c \cdot P \frac{\left(f_c - 1\right)^{G+1} - 1}{f_c - 2} \tag{1.1}$$

where f_c is functionality of the core, P – the spacer length and G is the generation number. It is obviously that number of monomers increases exponentially as a function of generation.

Finally, the multivalent ***surface*** is a third architectural part of the dendrimer macromolecule. It usually consists of reactive terminal groups, which number depends on dendrimer generation as follows:

$$n_G = f_c \cdot f_m{}^G \tag{1.2}$$

where f_m is functionality of the branching units. The reactive end-groups are composed of various chemical reagents that can be used for further functionalization of dendrimer. However, their number is still limited and includes only amine, amide, carboxylate, hydroxyl, methyl ester and several other compounds [36, 37]. In particular, the amine terminated dendrimers, which have a higher chemical reactivity compared to other chemical reagents, are commonly used for further modifications with various organic/inorganic

compounds. Since there is a huge amount of molecules that can be used to effectively functionalize dendrimer, their selection usually depends on individual demands. Furthermore, it is well known that the nature of end-groups determine physical and chemical properties (solubility, stability, shape and viscosity) of a given dendrimer family. Therefore, it should be relatively easy to control these properties according to the functional groups that dendrimers contain [38, 39]. Dendrimers with the functionalized periphery will be briefly discussed in more detail in 1.1.3 section.

In order to understand structural properties (shape, rigidity, segment density distribution in the molecule, *etc.*) of dendrimers more precisely it is still important to recognize how terminal groups are distributed within the macromolecule. For this reason, two models have been proposed to determine their localization in dendrimers. The first one suggested by de Genes and Hervet [40] was intended to show that the end-groups are grouped in concentric layers around the central core (an idealization of real dendrimer). Until now, survey of literature deals with this model, because (as we shall see later) that it offers a relitavely easy way to explain basic structure properties of dendrimers. However, more recent studies done by Lescanec and Muthukumar [41] as well as by Boris and Rubinstein [42], Ballauff and Likos [35], and other researchers, have predicted, and also confirmed a monotonic decrease in density when going from the center of dendrimer towards its periphery. According to their calculations, terminal groups of dendrimer are distributed throughout the entire volume, filling up the cavities and decreasing the functionality of the molecular surface. The latter model is more realistic and therefore plays a more important role in many researches of dendrimers.

As the dendrimer synthesis rely on iterative techniques where each successive layer is synthesized step-by-step, dendrimer ***size*** could be easily controlled during the synthesis. From a chemical point of view it seems relatively easy to extend dendrimer synthesis as long as necessary and to make macromolecule of a desired size. However, as it was predicted by de Gennes dense packing model [40], at a certain generation the growth of dendrimer

eventually reaches a critical point and due to the steric crowding of the branching arms its further increase into the higher generations is restricted.

Experimental investigations and molecular dynamics studies showed that the diameter of dendrimer *R* grows linearly as a function of generation *G*, whereas the number of terminal groups increases exponentially [43]. For this reason an occupied volume grows faster than accessible with generation increasing, and therefore dendrimer could reach only a limited generation number beyond which it is overdense and cannot fit in the physical space. The highest generation that can be achieved depends on dendrimer type and, according to Sheng et al., can be expressed as: $G_{\max} \sim \ln\left[f_m(P^3)/v \right]$, where *P* and *v* are length, and excluded volume of monomer segments [44]. Theoretical calculations of PPI and PAMAM dendrimers predicted the maximum volume they reach at G5 and G11 generations respectively [45, 46].

The strain hindrance not only influences dendrimer size, but also determines its ***shape***. Various experimental tools and molecular simulations revealed that the shape of dendrimer becomes more ordered (symmetric) when its generation increases (Fig. 1.3). As it was firstly predicted by Goddard theoretically [47] and by Goppidas et al. experimentally [48], the structure of the lower generation dendrimers is rather opened and floppy, but when generation increases – it becomes less deformable, more robust and symmetric. For example, when comparing dendrimers and polymers that both have equivalent sizes, it is easy to observe, that the shape of both materials will be different. Asymmetry of dendrimers decreases with increasing molecule size where in linear polymers it is almost unchanged [49]. Among many available experimental tools used for characterization of the dendrimer structure (these include AFM [50], TEM [51], ^{1}H NMR [52], hyper-Rayleigh scattering [53], *etc.*), X-ray and small-angle neutron scattering (SANS) are two techniques that have been proved to be an ideal tools for this purpose. When using both these scattering techniques it has been demonstrated that the PPI and PAMAM dendrimers of higher generations (G4 and G5) are perfectly arranged spherical

macromolecules, while being at the lower generations (G0 – G2) they posses two dimensional plain structure [43, 54, 55]. According to investigations performed by most researchers it was determined that the sizes of all dendrimers are limited and distributed in the range between 1 and 20 nm [45, 56].

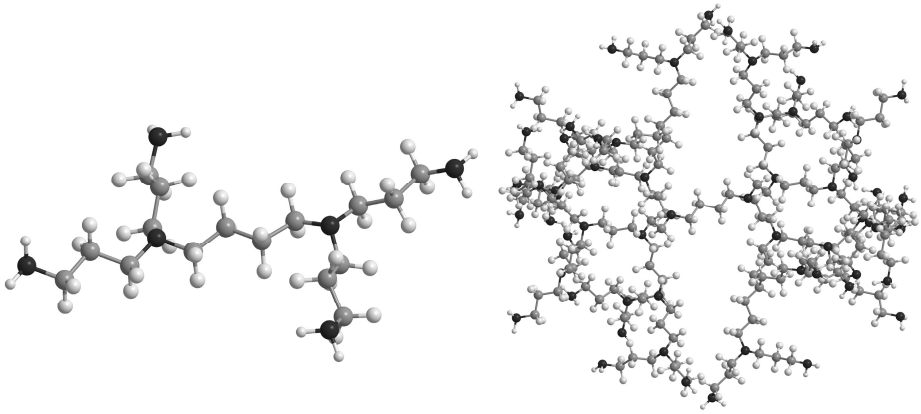

Fig. 1.3. Structure of the first (left) and fourth (right) generation amine-terminated PPI dendrimer.

Surface congestion also affects the formation of dynamic ***internal cavities*** within the higher generation dendrimers [57]. The dendrimers with densely packed surface may simply function as molecular containers (dendritic box) where drugs, genes, biological markers or other guest systems could be encapsulated [58-61]. They are also interesting substrates for metal nanoparticle synthesis, primary due to their uniform structure and ability to stabilize the nanoparticle surface against agglomeration [62]. Tremendous work in the synthesis of various types of nanoparticles within the dendrimers has been performed by Crooks [63- 65].

Although it is often argued that the structure of dendrimer is rigid, with uniform cavities, fixed molecule size and shape, the structure of real dendrimer may completely deviate from the spherical to the planar. Studies has shown that dendrimers are flexible, owing to deform or rearrange themselves [50]. Welch and Muthukumar have demonstrated that conformations of dendrimers

eventually depend on the solvent features in which molecule is dispersed [66]. For instance, amine terminated PPI and PAMAM dendrimers (they are both polar), in polar solvents may be fully expanded, reaching a maximum volume and almost spherical shape. However, in absence of the solvent or if polarity of solvent decreases, the volume of PPI and PAMAM dendrimers may collapse and its final shape will depend only on the interaction between dendrimer framework segments [26]. The molecular dynamics simulation studies performed on amine-terminated PAMAM dendrimers have shown that their conformations slightly depend on water acidity. At high acidities, dendrimer tend to conglomerate, whereas as pH decreases they become expanded [67]. In this way, conformations of dendrimer could be easily controlled depending on the solvent parameters [68, 69].

1.1.3. Functionalization of dendrimers

Rapid growth of dendrimer applications requests appearance of new types of dendrimers. The functionalization of specific positions in internal part of the dendrimers as well as the controlled functionalization of the dendrimer surface with different molecules is attractive for the development of new materials. The two principal ways, in which dendrimer macromolecules can be modified, are generally used in order to create new molecular compounds. Depending on both position and nature of functional units within the dendrimer macromolecule, monofunctional and multifunctional dendrimers could be distinguished [19, 18]. Monofunctionalization is a way in which only one type of molecules could be used to replace/functionalize only one architectural building block of dendrimer. However, multi-functionalization is a manner, allowing modification of whole dendrimer with different types of functional molecules [70]. Dendrimers functionalized by both methods are presented in Fig. 1.4.

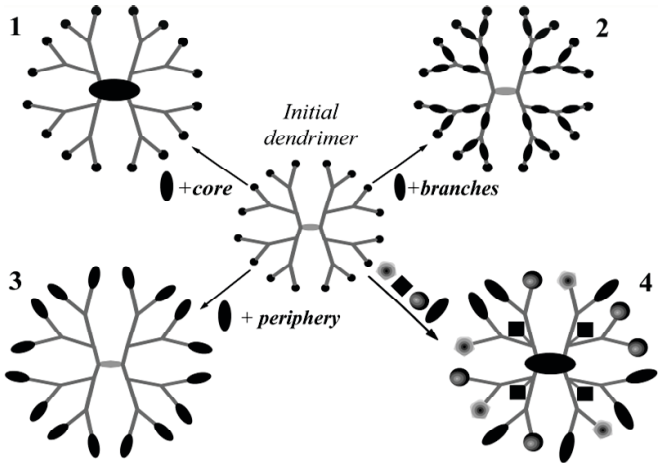

Fig. 1.4. Dendrimer functionalization ways. **1**-**3** examples presents mono-functional and **4** – multi-functional dendrimers.

Multifunctional dendrimers (see **4** compound in the Fig. 1.4), as well as other multifunctional macromolecules [71] have attracted considerable interest for their use in construction of various nanodevices, biomaterials, *etc*. For instance, dendrimers have been applied for theranostics after their modification with multiple functionalities consisted of targeting molecules, imaging agents and drugs [72, 73]. Also, dendrimers designed with electron-accepting molecule in the core and electron-donating on their branches were used to capture and store energy of light by moving electrons from the branches to the center of dendrimer [74]. Different generation dendrimers possessing coumarin-2 dyes at the periphery and coumarin-342 dye within their scaffold have shown efficient and fast (6 -18 ps) energy transfer from the periphery to the central part after the light irradiation. They have been considered as simple synthetic analogues of the natural light harvesting systems [75]. Binding of photochromic chromophores to dendrimer periphery, branches or into central part evokes large light-induced conformational changes of the whole macromolecule [2, 6, 76, 77]. Shibaev et al. has shown that dendrimers possessing two different types of photochromic groups on its framework undergoe dual photohcromism upon the light irradiation [71]. Although most

of these examples illustrate ineffable importance of multifunctional dendrimers, their synthesis is quite complicated and it becomes difficult to obtain high-quality materials.

Monofunctional dendrimers can typically be divided into three categories that are related by a difference in the position of attached molecules within the dendritic scaffold. These include dendrimers with functional core, functional branches and functional periphery. The best examples of monofunctional dendrimers correspond to **1-3** compounds presented in Fig. 1.4. Even though each architectural building block of the dendrimer was briefly described above (see Section 1.1.2), main properties of dendrimers with the peripheral functional groups in relation to the present thesis will be discussed in more detail.

The easiest way to the preparation of monofunctional dendritic systems is to functionalize the chemically reactive periphery of dendrimer. As it was already mentioned, there are only a several types of chemical reagents that can participate in reaction with a vast array of both homemade and commercially available compounds. Eventually, this leads to the development of dendritic polymers that may display a vide range of functional properties which can be tailored for specific applications [60, 78, 79].

During the last decade, there has been growing interest in the design of dendrimers in which the structural features and various physicochemical properties could be controlled by light [80]. Therefore, dendrimers containing photoactive terminal groups are particularly interesting due to their photoisomerization and tautomerization reactions [81], which suggests a possibility to control some of dendrimer properties by light. For instance, photoswitchable molecules experience changes in their hydrodynamic volume, size and polarity [82]. These processes may be applied to control some physical properties of dendrimers containing active terminal groups – orientation of their flexible branches, changes in their shape, volume, etc. Major emerging facilities of using this phenomenon are to form conditions for the guest molecule inclusion or release from the dendrimer. Dye, drug, or some

other molecules may be encapsulated or released by the appropriate dendrimer irradiation by light [6, 24, 61, 82-84].

The main physicochemical properties of the two types of functional groups that have been used for the functionalization of commercially available PPI and PAMAM dendrimers will be presented in the next section.

1.2. Organic photochromic materials and their features

1.2.1. Photochromism and photochemical reactions

Photochromic compounds

Photochromic phenomenon is known since the findings of Fritzsche in 1867, when the bleaching of an orange-colored solution of tetracene in the daylight and the recovery of the color in the dark was discovered [85]. Being a part of photochemistry, photochromism has received considerable attention in research only after the World War II. It is important to emphasize two significant reasons that encouraged interest in studying photochromic materials more precisely. First is directly related to the technological achievements. The most important role, primarily, was played by Eigen, Norrish and Porter, when they developed flash-photolysis technique, which, in turn, allowed detecting transient species in the very short lifetimes (at that date it was less than microsecond time resolution), and for that shared 1967 Nobel Prize in Chemistry [86]. Whereas, development of the ultrafast laser sources (reaching a femtoseconds time resolution *i.e.* 10^{-15} s) led to the birth of a new scientific field called femtochemistry. For research in the field of ultrafast chemical processes, using femtosecond laser techniques, Ahmed Zewail has received Nobel Prize in Chemistry in 1999 [87]. Another possible reason why photochromism becomes the focus of interest may be related to the achievements of modern computational chemistry [88].

Photochromism is generally characterized as a reversible reaction of the chemical species, induced in one or two directions by electromagnetic radiation, between two states with different absorption spectra [89].

Photochromic compounds are good examples of bi-stable molecular systems where geometrical structure, dipole moment, refractive index, dielectric constant and other physical or chemical properties could be controlled by light [90]. According to the back reaction mechanism, all photochromic materials are classified into the two main types: thermally stable and thermally unstable. If the back reaction occurs thermally, it is photochromism of "*T*" type (thermally unstable) and if photochemically – "*P*" type (thermally stable). Several examples of thermally unstable compounds are: anils, spyropyrans, azobenzenes *etc.*, meanwhile – fulgides, diarylethenes are thermally stable.

Laurent and Dürr have divided all photochromic materials into 13 different families with different types of photochemical reactions involved in the photochromic processes. [85]. Two examples of these materials will be presented in the further sections (see 1.2.2 and 1.2.3). Although the vast majority of photochromic compounds are synthetic by nature, several photochemical events can also be found in many biologically important systems [91, 92]. However, only bacteriorhodopsin and phytochrome remain photochromic being isolated from the living cell [90]. It is also important to mention, that photochromism is appropriate not only for organic materials, but it also takes place in inorganic and organic-inorganic hybrid materials. Several examples of latter compounds distinguishing photochromic properties are: Ag nanoparticles immersed into the TiO_2 matrix [93, 94], silver halides [95], rare earth metals [96] or transition metal oxides [97-99].

Photochemical reactions

It is well known that molecule has many excited states with several important differences between each other. Various photophysical and photochemical events could be involved in these energy levels upon the light interaction with mater. For instance, electronic transition caused by light absorption which lasts some 10^{-15} s; fluorescence, with lifetimes that are in the range from miliseconds to nanoseconds; internal conversion ($\sim 10^{-12}$ s); intersystem

crossing (10^{-12} - 10^{-9} s); energy transfer; various chemical reactions; *etc*. are several examples of these primary processes.

The events in which molecule undergoes conformational changes affected by light absorption of the electromagnetic radiation of ~600-120 kJ/mol molar energy are known as photochemical reactions [90]. Usually the lowest excited state (singlet S_1 or triplet T_1) lives long enough to take part in chemical reactions, because the upper energy levels (S_2, S_3, …, S_n, or T_2, T_3, …, T_n) are extremely short-lived and typically the non-radiative deactivation via internal conversion or intersystem crossing may occur primarily. On the other hand, photochemical reaction could be followed only if the lowest excited state lives long enough before molecule return back to the ground state resulting fluorescence.

Photochemical reactions, which take place after the photoexcitation of thermodynamically stable chemical species are common to almost all classes of organic compounds. So, it is significantly important to classify them by certain parameters. According to the number of participating molecules *unimolecular* and *bimolecular* photochemical reactions are possible. Depending on the nature of potential energy surfaces, three different unimolecular reaction mechanisms could be distinguished: adiabatic, diabatic and intermediate case (Fig. 1.5) [100, 101].

Adiabatic photoreactions occur when an electronically excited state of reactant is transformed to an electronically excited product and overall photochemical process occur entirely on the same, generally lowest excited electronic energy state *i.e.* energy is conserved within the reactive system. Thermal reactions usually occur adiabatically in the ground state. Another type of photoreactions are *diabatic*, they initiate in one of electronically excited state and end with the products in their ground state. During the diabatic process, energy is lost in the form of heat to the surrounding medium. Diabatic photochemical reactions are common to almost all condensed phase systems. There are also possible intermediate case photoreaction, when some reacting species escapes deactivation long enough to attain final product configuration.

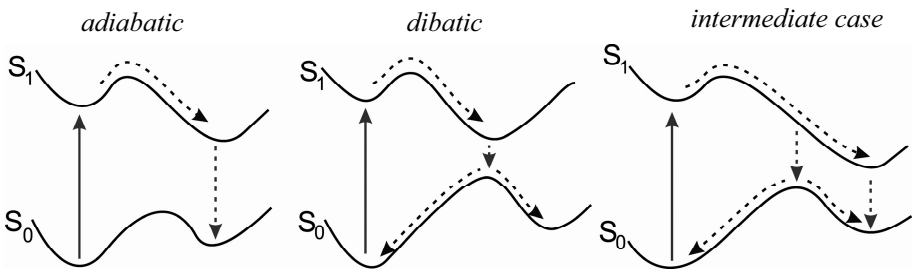

Fig. 1.5. Possible photochemical reaction surfaces.

Generally occurring unimolecular photochemical reactions are: i) *trans-cis* photoisomerization; ii) enol-keto tautomerization (intramolecular hydrogen/proton transfer) and iii) photodissociation.

The unimolecular photochemical reactions initiated in the lowest excited singlet states often have kinetics in the range from several tens of femtoseconds to hundreads of picoseconds [102]. For example, the first step in vision involving photoisomerization of the rhodopsin from its 11-*cis* to its all-*trans* isomer is complete in 200 fs or excited state proton transfer of anil type compounds are known to be the fastest events in the nature [103, 104]. The faster photochemical movements limited by vibrational motions and electron transfer are therefore not possible [105]. Due to the high rate of many photochemical processes, time resolved spectroscopy with a femtosecond time resolution is one of the most powerful tools for the direct view of the reaction profiles in photochromic systems. Among the vast majority of ultrafast spectroscopy techniques (these include femtosecond fluorescence upconversion technique, time resolved Raman, transient absorption spectroscopies, etc.), femtosecond transient absorption (pump-probe) is one of the most commonly used in the investigation of photoinduced dynamics behaviours [106].

Photochemical reactions inherent to the azobenzene and Schiff base containing compounds are shortly discussed in two further sections.

1.2.2. Photoisomerization of azobenzene-type compounds

Aromatic molecules possessing azo-group (N=N) with two phenyl rings are defined as azobenzene (*i.e. diphenyldiazene*) class chromophores. Azobenzenes and other compounds containing azo group have two isomers: thermally stable *trans* form and metastable *cis* form [107]. Their stability is determined by the spatial distribution of the phenyl rings. If the phenyl rings are on the same side of molecule (*cis* configuration), their electronic clouds interfere with each other – causing van der Walls (steric) strain, *i.e.* decrease of molecule stability. On the other hand, if the rings are at the opposite sides (*trans* configuration), molecule is more stable, because electronic clouds cannot interact. For this reason *trans* isomer is nearly planar, whereas due to the steric hindrance two rings of *cis* isomer are rotated of planar configuration at a 50° angle [108] (Fig. 1.6).

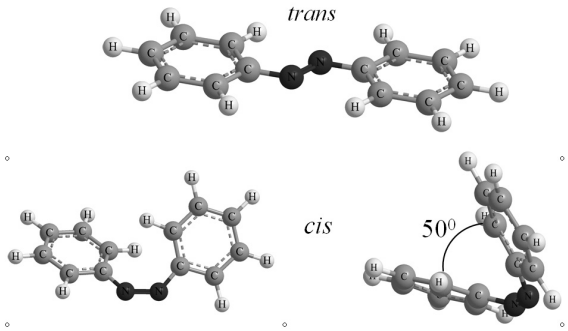

Fig. 1.6. Structures of the two azobenzene isomers.

The most exciting characteristic of the azobenzenes is their photochromic behaviour, mutually related with the efficient isomerization about the azo-linkage between the *trans* and *cis* geometrical isomers [109, 110]. For most azobenzene molecules, isomerization can be affected optically (*trans-cis*, *cis-trans*) and thermally (*cis-trans*) [111]. However, in some cases *trans* and *cis* forms can also be isomerized by resonant or inelastic tunneling of electrons [112] and electric field [113]. Isomerization reaction of azobenzenes is considered as ultrafast [114], fully reversible [115] and at the

same time one of the cleanest in the nature [116]. The distance between the para carbon atoms during isomerization reaction in azobenzene decreases from 0.9 nm in *trans* isomer to 0.55 nm in *cis* isomer (Fig. 1.7). These structure alterations usually leads large conformational changes in the molecular systems possessing azobenzene linkages [117].

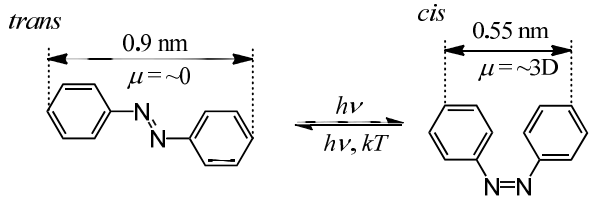

Fig. 1.7. Isomerization in azobenzene.

The early experimental and theoretical studies suggested that there is only one isomerization mechanism in azobenzenes: rotation around the central double bond or planar inversion. However, Rau and Luddecke have shown that both rotation and inversion are possible, and the way in which isomerization will take place depends only on the excitation wavelength [118]. As was shown, excitation to the π-π* results in isomerization via rotation about double N=N bond, similarly as in other photochromic well known compounds – stilbenes [7]. However, photoexcitation into n-π* absorption band leads isomerization via inversion about one nitrogen atom [119]. Two different azobenzene species and their isomerization pathways are clearly presented in Fig. 1.8.

Many azo-compounds exhibit unusual optical properties that are related to their geometrical changes. Each isomer shows two distinct electronic transitions: the strong π-π* absorption band in the near-UV and also low–lying *n*-π* band in the visible regions. Latter transition emerges due to the lone pair electrons that are localized on the nitrogen atoms. Both electronic transitions are allowed for *cis* isomer, whereas *n*-π* transition in *trans* isomer is forbidden, because the perpendicular excitation of an electron from the

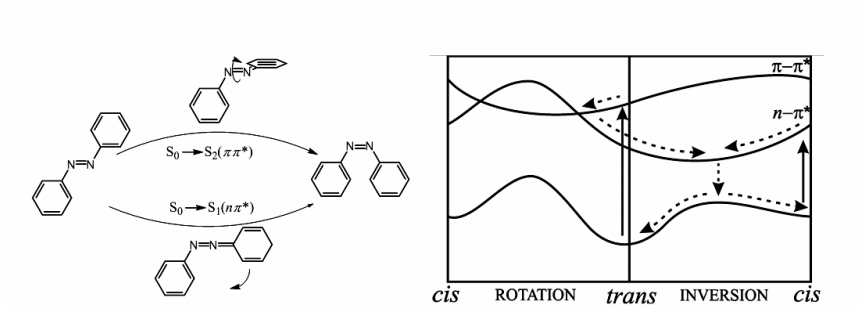

Fig. 1.8. *trans* – *cis* isomerization of azobenzenes and its potential energy surface, representing isomerization reaction at different excitation (Figure inspired on Ref. [120]).

nonbonding *n* orbital to antibonding π^* orbital is not allowed in the molecules with point group C_{2h} symmetry. For this reason intensity of π-π^* absorption band is higher for the *trans* isomer, whereas *cis* isomer has more expressed n-π^* band. It is worth to mention, that the position of the absorption bands slightly depends on the structure of the molecule and also on environment (solvent polarity, temperature, etc.). Therefore absorption spectra of azo-compounds could be tuned through the near UV – visible spectral region [121].

It is known, that azobenzene chromophores itself are generally nonfluorescent owning their ability to undergo *trans-cis* photoisomerization [122]. Nevertheless, observations performed by Struve indicated several exceptions and despite its low quantum yeld, fluorescence was detected firstly from n-π^* and several years later from π-π^* excited states of *trans*-azobenzene [123, 124]. Broad fluorescence band at long wavelength region (600-800 nm) appears after the excitation to the *n*-π^* state. Fujino has showed, that the two fluorescence bands of low quantum yield peaking at blue and red spectral regions are observed in *trans*-azobenzene after the excitation to its π -π^* absorption band [125]. Both they could be assigned to the emission from the π-π^* and *n*-π^* states. Emission from the π-π^* state was shown to be direct, whereas from *n*-π^* state it occurs after the internal conversion. Satsger has shown, that after the excitation of *trans* azobenzene at 488 nm, broad fluorescence band could be observed peaking at 640 nm with pronounced wing

in the red part. Whereas narrow fluorescence band peaking at 600 nm was observed from its *cis* isomer [126].

Since there are two pathways by which isomerization can occur, essentially important feature of photochromic compounds is their reaction dynamics, giving rise to the photochromic behaviour. Back-isomerization reaction (*cis-trans*), in absentia of external stimulation, in the ground state proceeds very slowly, because of the relatively high energy gap between both states (the energy minimum of *trans* isomer in pure azobenzene is approximately 0.6 eV below the *cis* isomer in the ground electronic state, whereas energy barrier between both isomeric forms is found to be about 1.6eV [127]). Typical back-isomerization lifetimes vary from milliseconds up to several days or even weeks [128, 129]. Undoubtedly, its rate depends on a large extent of a medium *i.e.* on the nature of the compound (substituents attached to azobenzene) and also on environment (pH, temperature, solvent). For instance, thermal *cis* to *trans* isomerization in azobenzene-centered dendrimer was observed over the course of approximately 3 h at room temperature [77]. As the thermal back isomerization of azobenzenes is very slow, in some cases it can be even more important to study slightly faster processes – initiated by photo-excitation. Fast photoisomerization dynamics of azobenzenes are relevant due to their possible applications in photooptical devices [106], biological systems [117], *etc*.

The fast photoisomerization mechanism and dynamics can be directly studied by time-resolved spectroscopy. The ultrafast photoisomerization dynamics of azobenzene derivatives were quiet well investigated both experimentally [114, 126] and theoretically [130]. It was observed, that isomerization dynamics from both π -π^* absorption is extremely rapid as the external EM stimulation is used. Therefore direct examination of present behaviour could be followed only using ultrafast spectroscopic techniques. Isomerization rate in different azobenzene containing compounds is slightly different, taking place from several hundreds of femtoseconds to several tens of picoseconds[114, 125, 130-132].

1.2.3. Phototautomerization of Schiff base containing compounds

Aldehydes and ketones react with primary amines to form imine – functional group that contains carbon-nitrogen double bond C=N. The imines obtained from the reaction of primary amines with carbonyl compounds are called Schiff bases. The first example of this compound was prepared by Hugo Schiff in 1864 [133, 134]. As well as azo-linkages, aromatic Schiff bases that form a large group of photochromes have also attracted considerable interest in photochemistry [135, 136].

Many physical and biological properties of Schiff base containing compounds are directly related to the presence of intramolecular hydrogen bonding which is responsible for the ground (GSIPT) and excited state intramolecular proton (hydrogen) transfer (ESIPT). The study of these chromophores is therefore relevant, because it allows us to understand naurally occurring events in chemical reactions as well as in large biological systems [137]**.** A great number of materials containing Schiff base functionalities reveal light induced reversible tautomerization. However, salicylidene aniline (SA) is perhaps the most widely investigated material of this class compounds. Being relatively simple in structure, SA is also generally used as a model compound in order to understand proton transfer behaviour from theoretical and experimental points of view, both in solutions and in films [135, 138-140].

Photochromic behaviour in aromatic Schiff base class compounds is simultaneously accompanied by the photoinduced structural changes based on enol-keto tautomerization and *trans-cis* isomerization. In aromatic Schiff bases, hydroxyl group is responsible for the H-donating properties, whereas nitrogen atom participate as H-acceptor. The most of Schiff base compounds exist as an enol form in the ground state, whereas upon the photoexcitation hydrogen is rapidly transferred to the nitrogen atom. Following conformation corresponds to *cis*-keto tautomeric form, which is more stable in excited state. Fluorescent *cis*-keto tautomer in picosecond time range isomerizes to the more stable *trans*-keto isomer by subsequent rotation around the C=N bond and finally it follows back proton transfer to the original enol tautomeric form. It

should be noted, that photochromic form is unable to undergo the reversible proton transfer unless the *cis* to *trans* isomerization takes place [141]. The typical scheme of tautomerization reaction in a simplest SA molecule is shown in Fig. 1.9. It is worth to mention, that the energy scheme is more or less similar to all anil type compounds.

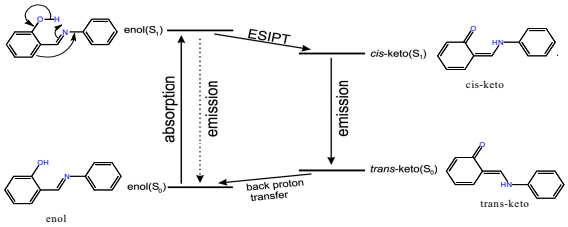

Fig. 1.9. Foster's cycle showing ESIPT reaction in simplest Schiff base containing compound Salicylidene-aniline.

The ESIPT is very rapid, because the transferring proton is near to the proton acceptor at the moment of excitation. The characteristic times of the ESIPT process was found to take place from the femto to the nanosecond time scale [135, 141, 142]. Moreover, proton transfer reaction rate and also photochromic behaviour of different aromatic Schiff base compounds were found to be dependent on the molecular conformations, attached substituents, physical state of the system and environment in which hydrogen bonds are embedded. Reaction rate decreases in hydrogen bonding solvents, because Schiff bases tend to form intermolecular hydrogen bonds with the atoms of the solvent. The proton transfer rates in SA have been observed to be 210 fs in cyclohexane and 380 fs in ethanol [138], or even less than 50 fs in [143].For example crystalline state usually slows down the chromophore formation due to the exciton effects.

2. Materials and experimental techniques

This chapter provides a detailed description of the materials and experimental setups employed in this study. In the first section of the current chapter, characterization of each investigated dendrimer, giving in consideration its structural formula and introduction to the synthesis, will be shortly presented. Whereas, detailed introduction of main techniques used in research is given in the second half of the chapter.

2.1. Investigated dendrimers

Amine terminated PPI and PAMAM dendrimers

Among the hundreds of composed dendrimer families, amine terminated PPI and PAMAM dendrimers appears to be the most extensively studied in the past twenty years [1, 144-146]. Possessing chemically reactive surface groups both they can be easily functionalized with dozens of different compounds and thus find widespread applications. For these reasons, PPI and PAMAM dendrimers in any case don't miss their interest to date. The chemical structures of both amine terminated PPI and PAMAM dendrimers are presented in Fig. 2.1.

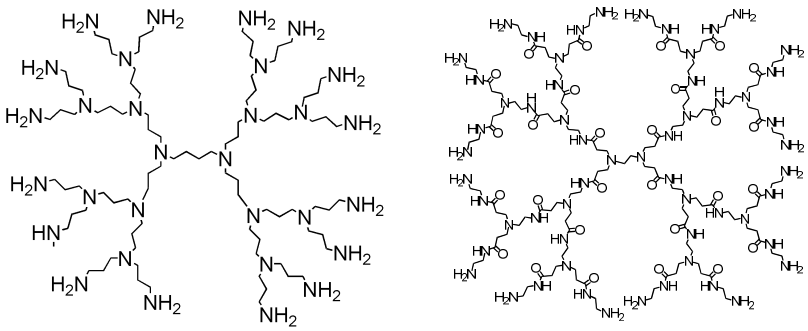

Fig. 2.1. Structural formula of third generation amino terminated PPI (PPI-NH_2) and PAMAM (PAMAM-NH_2) dendrimers.

Poly(propylene-imine) dendrimers

The synthesis of PPI dendrimers was introduced for the first time by Wörner [147] and Meijer [148] in 1993. Since then, PPI dendrimers have become commercially available in different companies. A divergent approach to the preparation of amine terminated PPI dendrimers is quiet well explicated and its full description could be found in the popular books on dendrimer chemistry [19, 149].

The structure of third generation amine-terminated PPI dendrimer is presented in Fig. 2.1a. As it could be seen, dendrimer is composed of three architectural building blocks: 1,4-diaminobutane core (DAB), consisting of four carbon atoms with two linked tertiary amine groups; short propyleneamine branching units containing only three carbon atoms; and primary amine functional groups at the periphery [148].

Poly(amidoamine) dendrimers

PAMAM dendrimers were firstly synthesized and commercialized by Tomalia [13] and Newcome [20] in 1985. They are considered as the first complete dendrimer family. As well as other dendrimers, they are also made of three distinct architectural building blocks. Ethylenediamine (EDA), composed of two carbon atoms with two tertiary amine groups, is usually used as an initiator core unit. The four branches bind to the central core are composed of four multifunctional amidoamine repeating units generally containing primary amine groups where two further branches could be attached.

Both PPI and PAMAM dendrimers closely resemble to each other, apart from a few differences. Diameter of both dendrimers of the same generation is relatively different. It is larger in PAMAM dendrimers, because their branches are much longer than those in PPI dendrimers. According to Crooks, thermal stability of PPI dendrimers is much higher than of PAMAM. PPI decompose at around 470˚C and it is almost four times higher than decomposition for PAMAM [150].

2.1.2. PPI-ESA dendrimer

PPI-ESA dendrimers were synthesized by condensation of 4-(4'-ethoxybenzoyloxy)salicylaldehyde (ESA) with the terminal amine groups of the different generation (G1-G5) poly (propylene imine) (PPI_NH_2) dendrimers, using a method described in refs. [151, 152]. Additional information related with dendrimer purity is also presented in ref. [151]. Structure of the third generation PPI dendrimer is shown in Fig. 2.2.

Primary amine terminated dendrimers in reaction with aldehyde (composite part of 4-(4'-ethoxybenzoyloxy)salicylaldehyde (ESA)) tend to form well know imine functional group, generally named as Schiff base (section 1.2.3). Reaction scheme of Schiff base formation within the amine-terminated PPI dendrimer is presented in Fig. 2.3.

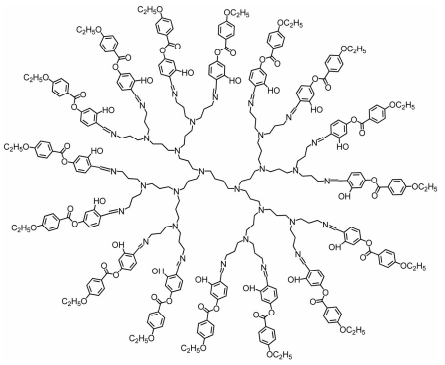

Fig. 2.2. Structure of G3 PPI dendrimer functionalized 4-(4′-ethoxybenzoyloxy) salicylaldehyde terminal groups. Generally named liquid crystalline dendrimers (LC-PPI).

In spite the fact that dendrimers have unusual liquid crystalline properties [151], they are also interesting because of the optical features, which will be presented in other chapters.

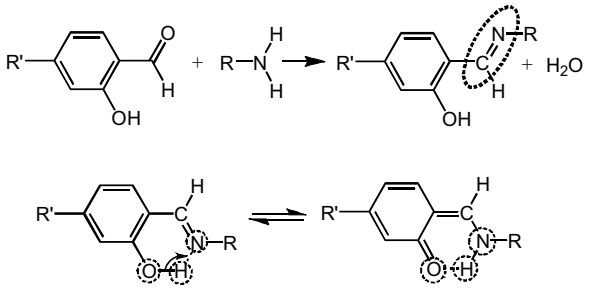

Fig. 2.3. Reaction scheme of PPI amine-terminated dendrimer with 4-(4'-ethoxybenzoyloxy)salicylaldehyde chromophore group. R' indicates the further dendrimer branches.

2.1.3. PPI-CAzPA and PAMAM-CAzPA dendrimers

Structures of the investigated PPI and PAMAM dendrimers functionalized CAzPA terminal groups are shown in Fig. 2.4. Obtained dendrimers were synthesized by connecting aromatic based 5-(4-cyanophenylazophenyloxy) pentanoic acid, designed as CAzPA to PPI and PAMAM dendrimers containing 16 terminal functional amine groups. Synthesis of dendrimers was described in detail in Ref. [153].

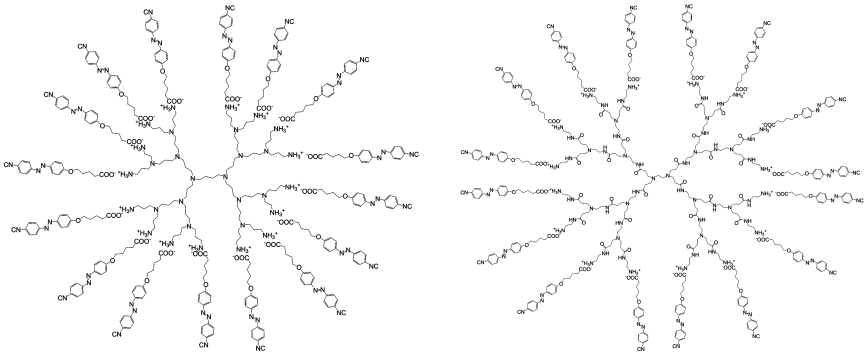

Fig. 2.4. Structure of PPI and PAMAM dendrimers functionalized with CAzPA. PPI-CAzPA and PAMAM-CAzPA.

2.2. Experimental methods

2.2.1. Atomic force microscopy

Atomic force microscope (AFM) is attributed to the wide family of scanning probe microscopes (SPM). It was developed in 1986 by Gerd Binning et al. [154]. The imaging of non-conductive samples is the greatest advantage of AFM compared with its antecedent – scanning tunneling microscope (STM). The possibility to measure biological materials, manipulate molecules and identify the strength of molecular interactions with sub-piconewton sensitivity gave rise to a real break through in the realm of AFM use [155].

Basic concept of AFM is schematically shown in Fig. 2.5. The most important part of microscope is a cantilever with a fine tip placed on its end.

Most commonly used probes are etched Si and carbon nanotubes. AFM measures the forces acting between a tip and a sample surface. Due to the attractive and repulsive forces, interactions between the tip and the surface will cause a positive or negative bending of the cantilever with picometer resolution. The bending is detected by reflecting a laser beam of the back of the cantilever to the position-sensitive photodetector. Therefore amount of the force between the probe and sample can be measured by converting them into the deflections of a spring according to Hooke´s law:

$$\Delta x = -\Delta F / k_c \qquad (2.1)$$

where the deflection Δx is determinated by the acting force ΔF and the spring constant k_c – which is determined by the tip parameters.

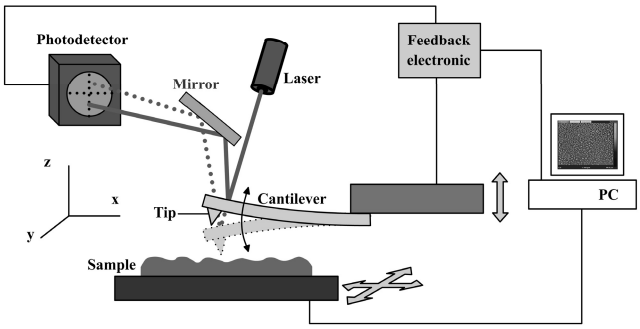

Fig. 2.5. Schematic diagram of the atomic force microscope.

Structure arrangement of the PPI dendrimers on Si and quartz surfaces was characterized by atomic force microscope (Dimension Nanoscope, VI, DI, Santa Barbara). In order to reduce needle interaction with material, all measurements were performed in tapping mode operation. In tapping mode, the cantilever oscillates close to its resonance frequency and interacts with the sample. Present investigation method is most commonly used for the structural measurements with AFM, because high (1-5 nm) lateral resolution and low damage to the samples may be achieved. However, it takes long time to measure the sample.

Preparation of dendrimer thin films for AFM

Depending on the desired properties of the thin films, a number of preparation techniques are developed, these include deposition from rapidly evaporating solvents, solvent coasting, Langmuir-Blodgett and many others. Spin coating is therefore one of the most widely used technique for the quick fabrication of thin films with a high structural uniformity on a various substrates (glass, silica or mica). Such thin film preparation method is relatively simple: particular amount of solution is covered on the sample and then for a certain period of time is rotated at an angular velocity ω in order to spread the solvent by centrifugal force. The film thickness D may be expressed as [156]: $D = \left(\eta / 4\pi\rho\omega^2\right)^{1/2} \cdot t^{-1/2}$. As could be seen, the tickness depends on angular velocity ω, solution viscosity η, its density ρ and even the spinning time t. One of the main disadvantage of this approach is that during the spinning one can waste a lot of material.

Four different solvents: dichloromethane, chloroform, tetrahydrofuran and toluene were used to prepare initial dendrimer solutions of concentrations $5 \cdot 10^{-3}$ M. The thin films of investigated dendrimers have been deposited on the square glass and Si substrates by spin coating solutions at room temperature at around 20˚C. The rotation speed i.e. 800 rpm for a period of 1 min was chosen. Information about the samples prepared for AFM imaging are summarized in Table 1. After the film deposition, all samples were left at the 50°C temperature for 5 h in order to stabilize the film during complete evaporation of the solvent.

1 Table. Detailed information about the samples, which were used for AFM investigations.

solvent / dendrimer	CHF	THF	Toluene	DCM
PPI-ESA of G1 and G5	Si	Si	Si	-
PPI-NH_2 of G1	-	-	-	Glass and Si

2.2.2. Steady-state absorption and fluorescence excitation

Steady-state absorption and fluorescence excitation spectra of the dendrimer solutions and thin films were recorded in the ultraviolet (UV) and visible spectral range from 200 to 700 nm. Absorption measurements were performed on a double-beam absorption spectrophotometer Perkin-Elmer Lambda 19 and excitation spectra was measured with a Perkin-Elmer LS 50B fluorimeter. Quartz cuvettes of different thickness (1; 5 and 10 mm) were used in both measurements. All steady-state measurements were performed at room temperature.

2.2.3. Steady-state and time-resolved fluorescence

Fluorescence spectra and fluorescence decay kinetics were measured using Edinburgh Instruments Fluorescence Spectrometer F900. Picosecond pulsed diode laser EPL-375 emitting 50 ps duration pulses was used for samples excitation. The average excitation power was about 150 μW. In every experiment fluorescence spectra was corrected for the instrument detector sensitivity. The time resolution of the setup, by applying apparatus function deconvolution, was about 100 pc. The pulse repetition rate was 10 MHz and the average excitation intensity was about 100 $\mu W/mm^2$. In contrast to steady state absorption and fluorescence excitation measurements, fluorescence spectrometer has been equipped by liquid helium cold finger cryostat (Janis CCS-100/204) for the solvent and film measurements at lower than room temperatures.

Streak Camera

Fluorescence lifetime measurements were also measured by using electrooptic streak camera. Electrooptic or more commonly known as “streak” camera is an instrument used to direct measure of an ultrafast light pulses in the time domain. The device simultaneously provides information about three parameters: fluorescence intensity and its relaxation time at different

wavelengths. Time resolution of most commercially available streak cameras is at around several picoseconds or even less.

The time resolved photoluminescence have been measured according to the setup shown in Fig. 2.6. One part of the scheme composed of monochromator – streak camera – CCD is always fixed. However, another part equipped by the lenses and sample could be changed during the experiment.

The Nd:YAG laser used for the sample excitation operates at 80 MHz repetition rate generating 12 ps duration pulses at $\lambda = 1064$ nm. Whereas third-harmonic laser radiation $\lambda = 355$ nm was used for sample excitation. Laser light passing through the lens (L1) is focused onto the sample where it initiates photoluminescence. Fluorescence scattered from the sample is collected by the pair of the quartz lenses (L2 and L3) and focused into the monochromator.

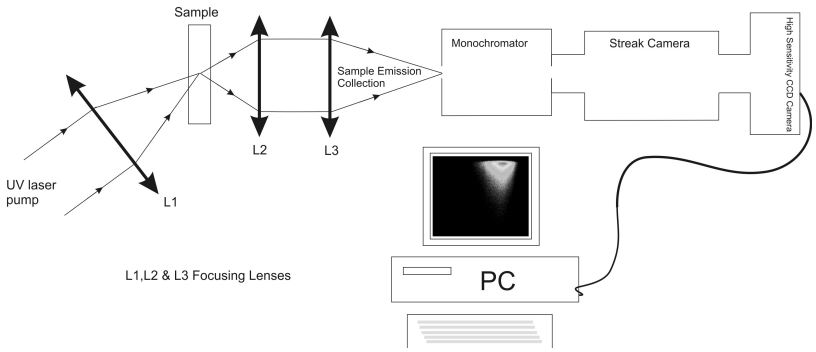

Fig. 2.6. The diagram of the experimental time resolved fluorescence setup equipped by streak camera.

Operating principle of streak camera is presented in Fig. 2.7. As the fluorescence light, emitted from the UV-irradiated sample, enters the photocathode, photons are instantly converted into photoelectrons. Their number is proportional to the intensity of an incident light. These photoelectrons sare further accelerated by the electric field which is created between two accelerating electrodes and then passes through the deflection system. A high voltage is applied to the electron deflection system and electrons are conducted to the phosphor screen at different angles according to the time when they arrive on to the photocathode. When the electrons hit the screen they changes back to the photons to create a brief instant of light.

Fluorescent pattern composed on the screen is recorded by charge coupled device (CCD) resulting streak pattern which is analyzed with a special imaging software. Time resolved

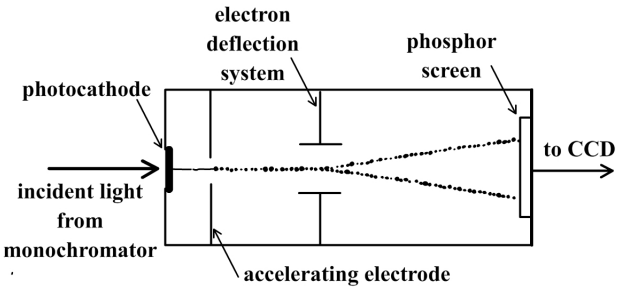

Fig. 2.7. Schematic view of streak camera.

2.2.4. Ultrafast transient absorption spectroscopy

Most of the experimental observations within the thesis have been carried out by means of conventional femtosecond transient absorption spectroscopy, which is usually referred to as a pump-probe. The typical scheme of transient absorption setup is shown in Fig. 2.8. Spectrometer is based on the amplified femtosecond Ti: Sapphire laser Quantronix *Integra-C* generating 130 fs duration pulses at 810 at the 1 kHz repetition rate. The main laser radiation was splitted into the two light channels (*Ch-1* and *Ch-2*). The radiation from the first channel (*Ch-1*) is directed to the parametric generator TOPAS-C, which is used for the excitation pulse wavelength tuning. After that, radiation of a certain wavelength passes through the chopper and hits the sample (S) where it initiates photochemical reaction or physical change.

Radiation in the second light channel (*Ch-2*) is used for probing the sample. First of all, probe pulse passes through a delay line which changes its delay according to the excitation pulse and then falls into the sapphire plate (SP). Although the pulse energy is not very high, its peak power is sufficiently large, because it is inversely proportional to the pulse duration: $P = E/t$. Considering, the fact that t is about $\sim 10^{-13}$ s, and E is in order of several mJ, the

rate of energy which is in order of 10^{10} W in every pulse may be achieved. Such high amount of energy upon the interaction with a medium can easily create numerous nonlinear phenomena. One of such phenomena is a white light continuum which in present setup is generated by focusing fundamental radiation to the 2 mm thick sapphire plate (SP). The white light continuum spreads in to the broad spectral range, typically from UV to near IR. By using beam splitter, continuum radiation is divided into the two equal parts: probe and reference pulses. The probe pulse is focused on the sample (S) in such way to overlap with the excitation pulse. Whereas reference pulse unhinderly passes through the sample near the probe. Both pulses, probe and reference, are therefore focused into the monochromator and by changing the probe detection wavelength, transient absorption spectra could be measured.

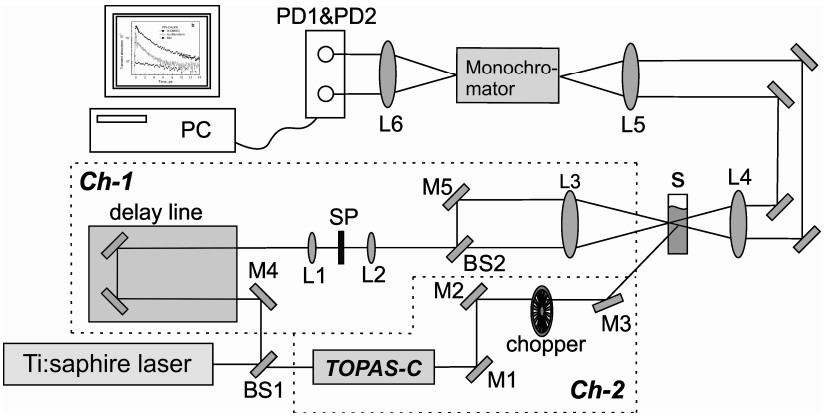

Fig. 2.8 Experimental setup for transient absorption measurements.

The excitation beam of particular frequency is periodically chopped. Therefore, induced optical density change is calculated according to the probe and reference beam energies, measured at a certain wavelength, with and without sample excitation [120]:

$$\Delta al = -\lg\left(\frac{I_p}{I_0}\right)_{exc} + \lg\left(\frac{I_p}{I_0}\right)_{nonexc} \tag{2.3}$$

Where I_p is intensity of probe pulse and I_o – intensity of reference beam.

During the measurements group velocity dispersion was compensated by simultaneously moving a delay line. In order to avoid induced absorption anisotropy effects the probe polarization was adjusted to 54.7° relative to pump pulse polarization.

3. Optical features and AFM imaging of PPI dendrimers

This chapter is devoted to the study of surface morphology of the functionalized PPI dendrimers and also to the optical study of amine-terminated PPI dendrimers in dichloromethane. The surface rigidity and layer formation peculiarities as well as optical absorption features will be discussed in more detail.

3.1. Characterization of PPI dendrimer surfaces by AFM

The controlled self-organization related with non-covalent interactions (H-bonding, Van der Waals, electrostatic and other forces), opens way to create periodically arranged or even disordered nanocomposities consisting of the various types organic materials**.** It appears, that due to their unique structure and a huge amount of active functional units, dendrimers are essentially important for the numerous applications ranging from drug delivery to structure materials: light emitting diodes or Solar cell devices [157, 158]. Because of many emerging applications molecular solids are usually used in the form of the films, it is a critical need to understand structure of dendrimer in solid state. Atomic force microscope is an ideal instrument suited to provide a high-resolution imaging and measurements of surface topography.

Typical AFM height images of the first generation amine terminated PPI dendrimer thin films spin coated on Si wafer and glass substrates are shown in Fig. 3.1. As it can be seen from the figures, both dendrimer samples have slightly different surface morphology. The amine terminated PPI dendrimer deposited on the glass substrates tend to form almost uniform layers with the low surface roughness <15 nm (Fig. 3.1a and b). In spite of this, only a single aggregates of several tens of nanometers in diameter may be observed within entire 100 μm^2 thin film area. These sparsely distributed aggregated reaches or even exceeds 15 nm heights.

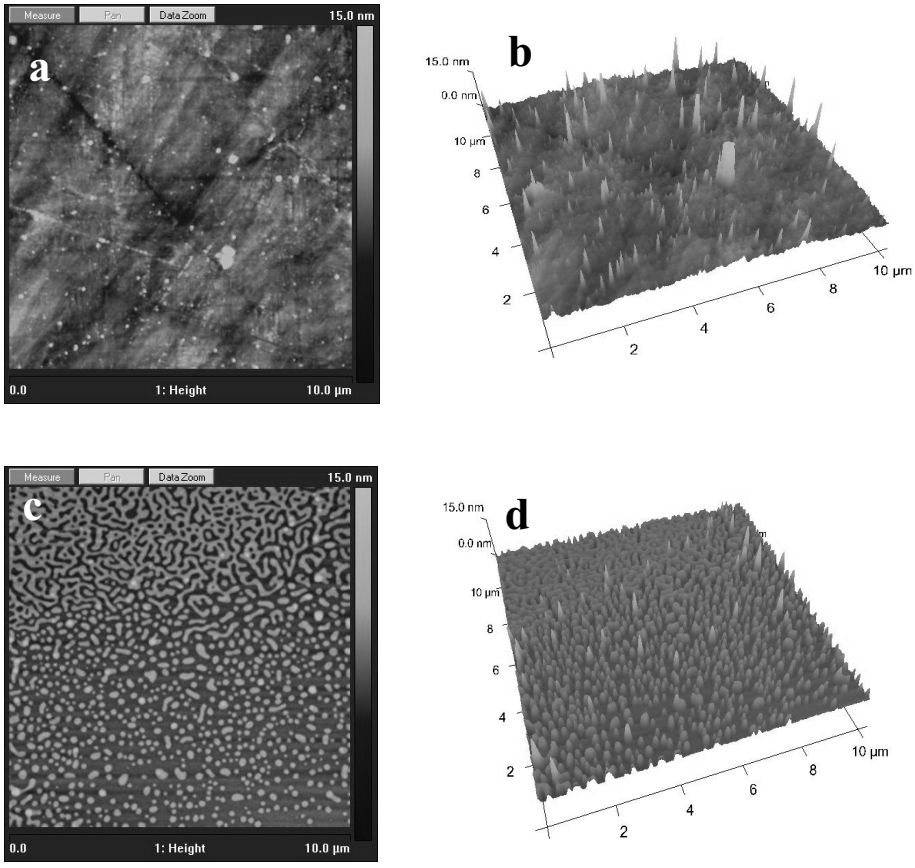

Fig. 3.1. AFM images of a 10 µm by 10 µm area of the first generation amine terminated PPI dendrimer obtained on silica (a, b) and glass (c, d) substrates.

The same dendrimer on Si substrate forms tightly packed aggregates (Fig. 3.1c and d). However, looking to the figures more accurately, we can see that surface morphology can vary at different parts of the sample. Single cylinder-form aggregates with diameter of about 100 nm are more pronounced in the lower part of the Fig. 3.1c and d. Meanwhile significant differences are clearly seen in the upper part of the same figures, where high-dense aggregates form nearly ordered structures. Present thin film inhomogeneity may be caused by the slow rotation and even fast solvent evaporation rate [159].

It is not surprising that both dendrimer films have slightly different surface morphology, because surface roughness depend not only on the

peculiar properties of dendrimers, but also on the type of substrate which is used for thin film deposition [160]. It is probably the main factor which determines the morphological differences between the amine terminated PPI of dendrimers.

Surface morphology of PPI dendrimers functionalized by ESA terminal groups are shown in Fig. 3.2. PPI-ESA dendrimer thin films were prepared only on the Si substrates, because investigations performed with amine terminated PPI dendrimers revealed better thin film coating quality on Si. Thin films of G1 and G5 dendrimers coated from chloroform solution are shown in Fig. 3.2a, b, whereas the films deposited from the same dendrimer dissolved in THF and toluene are presented in Fig. 3.2c, d respectively.

AFM micrographs of PPI-ESA dendrimer films formed by spreading chloroform solutions indicate that surface morphology between G1 and G5 dendrimers are completely different. AFM image of the first generation dendrimer displays structural organization of dark and bright regions (in the background) corresponding to the valleys and hills. The short spacing between the small hills/valleys is of several tens of nanometers. A small number of larger aggregates are also clearly visible in the G1 dendrimer films. Aggregation in PPI-ESA films by analogy with PAMAM dendrimers deposited on mica surface [50], may also be affected by high solvent concentration. This indicates that PPI-ESA dendrimers tend to form a densely packed film on Si surface in order to maintain lower surface tension. Whereas, excess of the dendrimer then aggregate on the thin film surface to produce a globular structure.

These globular structures in the fifth generation dendrimer film are distributed in whole 25 μm^2 area and form large islands reaching even half of micrometer (Fig. 3.2a and b). Also, the small valleys and hills are no longer visible in G5 dendrimer, since they form excrescence chains girthed around these aggregated dendrimer clusters. The cluster height is relatively small and reaches only ~ 3-4 nm.

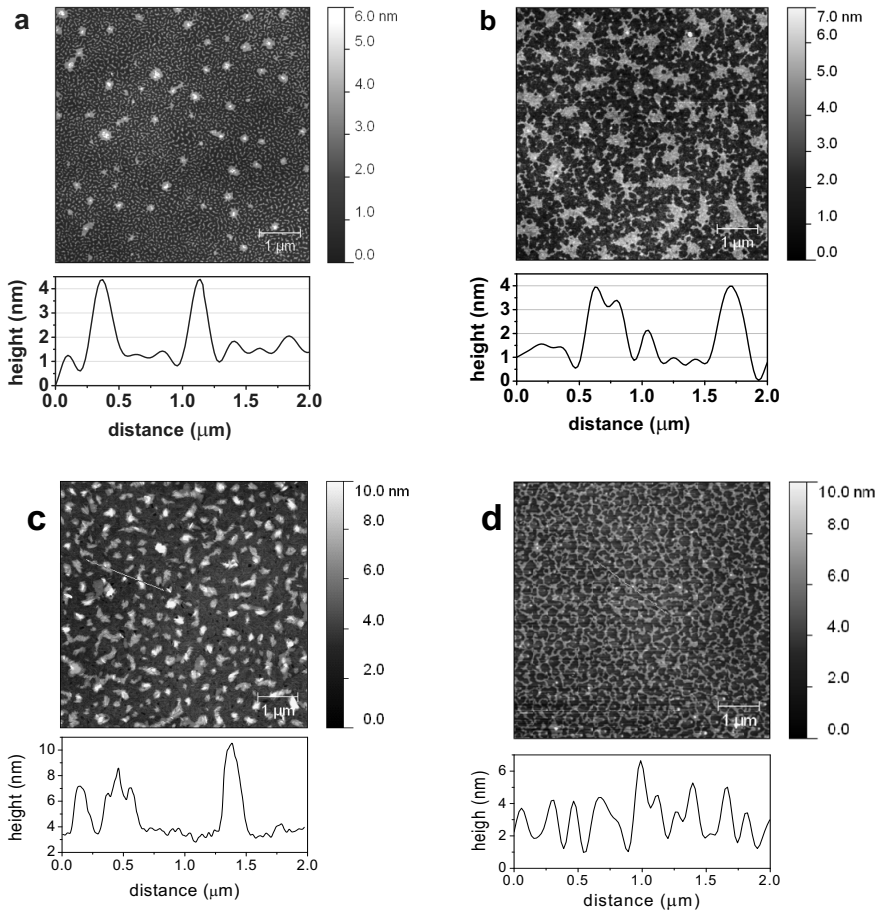

Fig. 3.2. Tapping mode AFM images of a 5 μm by 5 μm area of the PPI dendrimer thin films deposited on Si surface. (a) G1 from chroroform solution; (b) G5 from chloroform solution; (c) G1 from THF solution; (d) G1 from toluene solution.

During the preparation of the PPI-ESA dendrimer thin films on Si substrates, we also investigated three different solvents to depict their influence on the surface morphology. AFM micrographs of the G1 dendrimer films deposited from three characteristics solvents, including CHF, THF and toluene (section 2.2.1) are presented in Fig. 3.2a, c and d. It is obvious that the film morphology highly depend on the solvent from which it was deposited. Specifically, film cast from THF exhibit large grains that span several hundreds nanometers. Their thickness is approximately twice larger than in films prepared from toluene and chloroform solvents and reaches ~ 6 nm height. Consequently,

rough film tendence to crystallize is present, if PPI-ESA dendrimer in toluene is dissolved. Although in most cases surface roughness increases with increasing vapor pressure, it is not really true for the films coasted from THF and toluene, because obtained results are opposite to that which were observed by other authors [161]. The film deposited from toluene is relatively rough and has more structural rearrangement than the films obtained from CHF and THF. Because, toluene has boiling temperature at 110˚ C, whereas CHF and THF at 61.2˚ C and 66˚ C respectively, the ordered rearrangement may be influenced by the slow solvent evaporation rate [162].

3.2. Absorption and scattering in PPI amine-terminated dendrimers

Steady state absorption of commercially available amine-terminated dendrimers of generations G1-G5 were studied in UV-vis spectral range. The gel-like substance of dendrimers was dissolved in dichloromethane. The obtained solutions (pH 8) for generations G1 and G2 were transparent whereas significant light scattering was observed for G4 and G5. The transmission of freshly-prepared solutions did not change during several hours.

Typical optical absorption spectra of the optical density for first generation (G1) of amine-terminated PPI dendrimer solutions in dichloromethane at various concentrations are presented in Fig. 3.3. The spectra characterize the total transmittance loss due to the absorption and scattering of light when passing the dendrimer solution. As is seen, the absorption band at 270-290 nm is quiet well resolved. The band intensity was found to increase linearly with an increase of

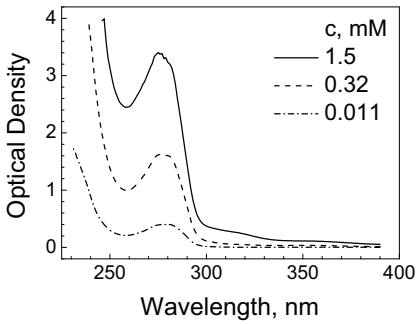

Fig. 3.3. Spectral dependence of the optical density of PPI amino terminated dendrimer (G1) solutions in dichloromethane at various molar concentrations *c*.

the dendrimer molar concentration at low concentrations of order 1×10^{-5} M. A weak band peak at about 315 nm was also detected at higher dendrimer concentrations. An occurrence of the absorption in the long wavelength region at 360 nm has been also noticed in the solutions of amine (NH_2) and carboxylate ($-COO^-$) terminated PAMAM dendrimers of a higher concentrations (8.6×10^{-5} M) [163]. Below, we shall pay the main attention to the regularities in the optical spectra related to the peak at ~270-290 nm.

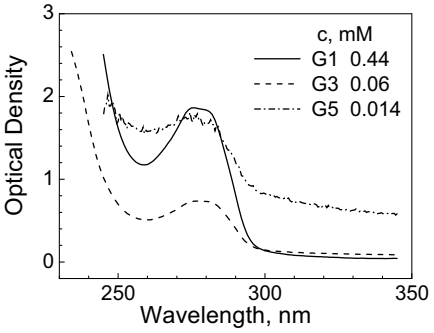

Fig. 3.4. Spectral dependence of the optical density of PPI amino terminated dendrimer solutions in dichloromethane at constant weight concentration 0.1 mg/mL correspond-ing to various mole concentrations *c* for generations G1, G3 and G5

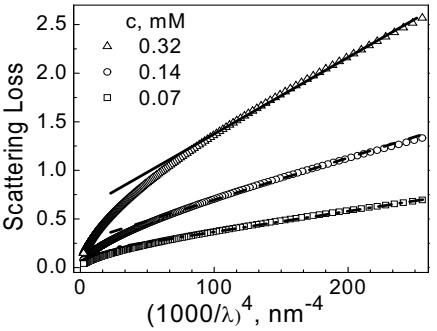

Fig. 3.5. Scattering loss, *i.e.*, the optical density with absorption contribution excluded, versus λ^{-4} at various molar concentrations of amino terminated PPI dendrimer (G5) solutions in dichloromethane.

The variation of the optical spectra of amine-terminated PPI dendrimers of various generations is illustrated in Fig. 3.4. The spectra of solutions of the same weight concentration (0.1 mg/mL) and hence of various mole concentrations are shown for generations G1, G3 and G5. As in Fig. 3.3, the optical density has been measured in transmission mode and corresponds to the extinction represented by the contributions of both absorption and light scattering. As is seen in Fig. 3.4 at longer wavelengths (λ>330 nm) the transmission losses are coused by dominating scattering. Where of the high surface activity amine terminated dendrimers tends to aggregate at very low concentrations. Therefore light scattering which was observed at the higher generation dendrimers may be affected by dendrimer aggregation [164].

The influence of ligh scattering increased for larger generations G4 and G5. The dominating contribution of light scattering for dendrimers solution of generation G5 is clearly illustrated in Fig. 3.5, in which the losses due to absorption have been excluded. As is seen, the spectral dependence of scattering losses agrees well with Rayleigh scattering law. A linear dependence of scattering loss versus λ^{-4} was observed in a wide spectral range with the slope increasing for higher dendrimer concentrations through some influence of background absorption was still evident. An increase of light scattering in dendrimer solutions of higher generations is well understood taking account into a corresponding increase of viscosity [165] and the phase behaviour in amine-terminated dendrimer solutions [166].

For a spherical particle of the diameter *a*, which is smaller by several orders of magnitude than the wavelength λ of incident electromagnetic radiation, the intensity the intensity I_s of light scattered from a beam of unpolarized light of intensity I_i is given by a well known formula for Rayleigh scattering [167]:

$$I_s = \frac{16\pi^4 a^6}{r^2}\frac{1}{\lambda^4}\left|\frac{m^2-1}{m^2+2}\right|\left(1+\cos^2\theta\right)I_i \qquad (4.1)$$

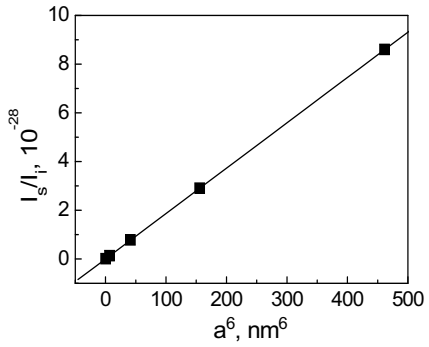

Fig. 3.6. The relative intensity I_s / I_i of Rayleigh scattering calculated according to (1) versus a^6 (where a is the diameter of dendrimer) for PPI dendrimers of generations G1 to G5 in dichloromethane at λ=400 nm.

where *m* is the refractive index of the dendrimer molecule, θ is the scattering angle and *r* is the distance to the particle. Taking into account the radius of the particles for PPI dendrimer generations G1 to G5 [168], the relative intensity of Rayleigh scattering (Fig. 3.6) was simulated using the MiePlot v.4.2 software [169]. The calculated results of the Rayleigh scattering at

the 400 nm, where anny significant absorption band of dendrimer wasn't observed, by dendrimer particles are shown in Fig. 3.6. The simulated results are in agreement with the experimentally observed light scattering data.

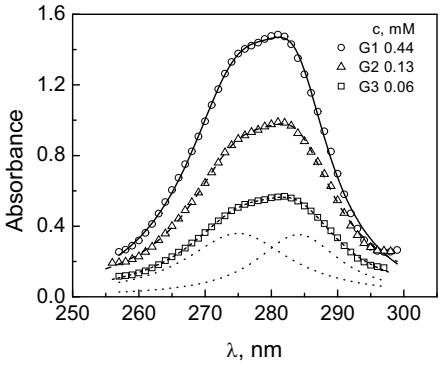

Fig. 3.7. The experimental (points) and decomposed (curves) absorbance spectra, *i.e.*, the optical density the scattering contribution excluded, of amino terminated PPI dendrimers of generations G1, G2 and G3 at constant weight concentration 0.1 mg/mL corresponding to various mole concentrations *c*.

The fine structure of the absorption band at 270-290 nm for PPI dendrimers was analyzed in the model of Lorentzian-type lines. In this spectral region, two peaks were clearly resolved (Fig. 3.7). The Lorentzian-type components of width 20 and 14 nm were observed at 275 and 284 nm, respectively. It should be notted that double band structure was also determined in the absorption spectra of a series diaminoalkanes [170].

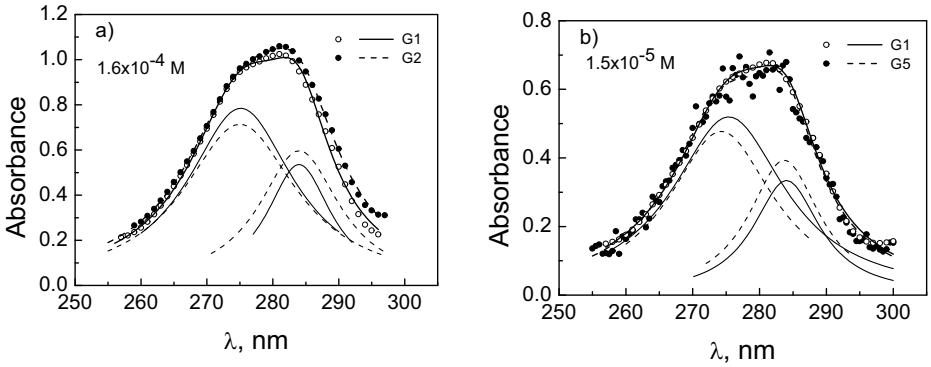

Fig. 3.8. The experimental (points) and decomposed (curves) absorbance spectra of amino terminated PPI dendrimer for generations G1, G2 and G5 at higher (a) and lower (b) molar concentrations

The line-shape of components in the double band was similar for all dendrimer generations. Figure 3.8 illustrates the fine structure of the double absorption band of amine-terminated PPI dendrimer solutions in

dichloromethane. As is seen, the double band structure is close for various generations under consideration at the same molar concentrations. Thus, it is reasonable to assume that the excitation involving core is responsible for the absorption in the UV double band

3.3. Short summary

The effects of dendrimer molecular weight, substrates and solvents conditions on the morphology of the films prepared via spin coating were investigated. Morphological differences between amine terminated PPI dendrimer films deposited from dichloromethane on the Si wafer and glass are influenced by substrate roughness. Despite the low thin film inhomogeneity, originated during the preparation, higher thin film order was obtained on the Si substrate, suggesting that smoother amine terminated dendrimer films it is better to prepare on Si substrate.

Significant difference observed in the morphology of PPI-ESA dendrimers demonstrate the importance of dendrimer generation and solvent choice during film fabrication.

The absorption spectra of amine-terminated PPI dendrimers of generations G1-G5 dissolved isn dichloromethane were measured and analyzed. The results of quantum mechanical calculations agree well with experimental data in the region 270-290 nm of the double band, which is typical of amin-terminated PPI dendrimers. The fine structure of the double band is similar for all generations under investigation and is due various types of optical transitions involving branched interiors and periphery. It was also found that the role of the Rayleigh-type light scattering significantly increased for higher generations G3-G5.

4. Excited state relaxation in PPI and PAMAM dendrimers functionalized with CAzPA terminal groups

In this section steady-state and femtosecond time resolved UV-visible transient absorption spectroscopy has been applied for investigation of the third generation poly(propylene-imine) PPI-$(NH_2)_{16}$ and second generation poly(amido-amine) PAMAM-$(NH_2)_{16}$ dendrimers with substituted azobenzene derivatives 5-(4-cyanophenylazophenyloxy) pentanoic acids (CAzPA) as terminating groups (see Fig. 2.4). Dendrimers in solutions and in solid films were addressed. We show that the dendrimer structure has minor influence on the isomerization reaction in solutions, while in a solid state the isomerization reaction becomes slightly slower.

4.1. Steady state absorption and fluorescence

The steady-state absorption and fluorescence spectra in UV-visible spectral range of PPI-CAzPA and PAMAM-CAzPA dendrimers in chloroform and DMSO solutions are presented in Fig. 4.1. The obtained absorption spectra contain two main absorption bands situated at about 360 nm and 450 nm. Those absorption bands shall be attributed to the CAzPA terminating groups [171]. Similar spectra have been also observed for pure nonsubstituted azobenzene in hexane [114] [125], only the short wavelength band of dendrimers is shifted by about 40 nm to the long wavelength side. The weak long wavelength band appears approximately at the same position. Evidently, substitutions and dendrimer cores connected through the oxygen atom do not significantly affect electronic properties of azobenzene moiety. By analogy with the absorption spectrum of azobenzene the first strong band in UV region at about 360 nm shall be assigned to the symmetrically allowed π-π^* transition and the second low intensity band near the 450 nm to the n-π^* transition [172]. As it was previously discussed (Section 1.2.2.) the n-π^* transition for the *trans* form is symmetrically forbidden [171], hence the low energy absorption band is very weak. Position of the high energy band is completely identical for both

dendrimers and in both solvents despite of their different polarity and dielectric permittivity. This is in agreement with the absorption spectra of azobenzene, which is also almost insensitive to solvent [173].

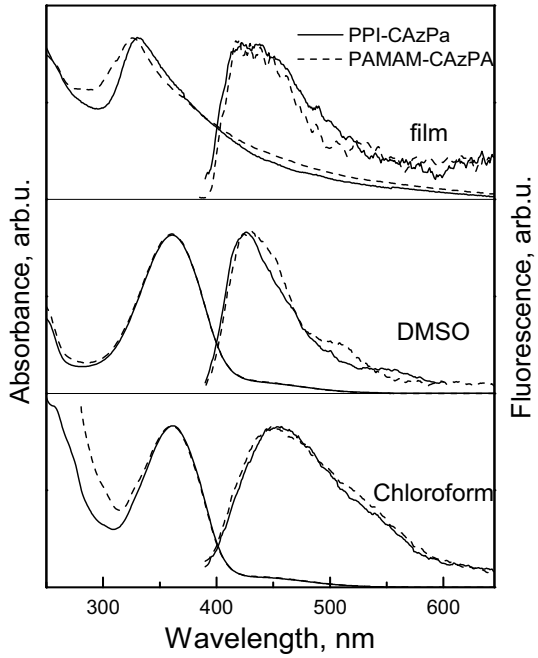

Fig. 4.1. Absorpion and fluorescence spectra of the PPI-CAzPA and PAMAM-CAzPA dendrimers in chloroform, DMSO solutions and in film.

Absorption spectrum of the dendrimer film is significantly different. The high energy π-π* absorption band is shifted to the short wavelength side by about 30 nm and 34 nm for PPI-CAzPA and PAMAM-CAzPA dendrimers, respectively. The shift of the absorption band may be related either to the different chromophore interactions with solvent in solutions and with other dendrimers in solid films or to chromophore-chromophore interactions. The former seems to be unlikely because the band positions, as discussed, are almost insensitive to solvent parameters. The chromophore-chromophore interactions may become important in densely packed solid films. CAzPA groups probably arrange in the solid state to form plane-to-plane type

aggregates, which due to excitonic interactions have blue shifted absorption [172]**.** The broad long wavelength absorption band edge is evidently partly an artifact caused by the light scattering in the inhomogenous solid film. The n-π^* absorption band, if it is presented in solid film, is hidden under the droad light scattering spectrum.

Only a very weak fluorescence with the quantum yield of the order 0.1 % was detected for both dendrimers in both solutions under their excitation at 375 nm. However, the fluorescence spectrum slightly depends on the solvent; it is wider and red-shifted by about 25 nm in chloroform solution. Similar weak emission has also been observed in trans-azobenzene solution in DMSO [126]. Generally, azobenzenes show very weak fluorescence under excitation to both n - π^* or π - π^* states [173]. Position of the main fluorescence band allows its attribution to the π - π^* transition. The long wavelength corresponds to n - π^* transition. Appearance of the n - π^* fluorescence of azobenzene after excitation to π - π^* state was briefly discussed by Fujino [125]. Dendrimer film also show very weak fluorescence with spectra similar to that in the chloroform solution. The fluorescence of PPI_CAzPA dendrimer thin film was also measured at different temperatures in the range from 335 to 150 K (Fig. 4.2). Low temperatures can have an essential effect on the photochemical reaction, because it can suppress many photochemical processes making conditions to complete fluorescence. Nevertheless, even at low temperatures, increase of fluorescence intensity was slightly low. The peak position centered at around 430 nm was also insensitive to temperature changes.

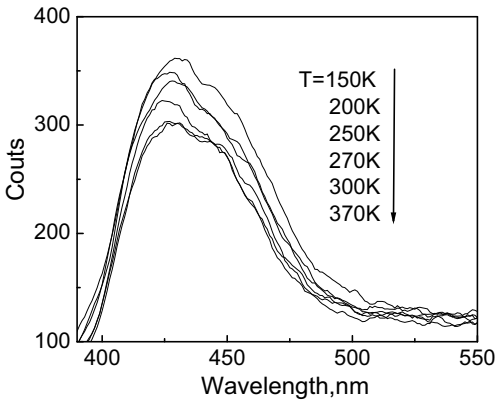

Fig. 4.2. Fluorescence spectra of the thin film of PPI-CAzPA dendrimer at different temperatures.

Fluorescence decay kinetics measurements were also performed, however fluorescence lifetime both in solution and in films is very short, much shorter than the time resolution of setup.

4.2. Time resolved spectroscopy of PPI and PAMAM CAzPA

Excited state relaxation dynamics of dendrimers in solutions and in films has been investigated by means of the femsosecond time-resolved transient absorption spectroscopy. Differential absorption spectra of the PPI-CAzPA dendrimer in DMSO solution at different delay times are shown in Fig. 4.3a. The spectrum was measured after the sample excitation close to the absorption maximum at λ=350 nm, which corresponds to the π-π* electronic transition. A broad induced absorption band is evident at all delay times. The shape of the induced absorption spectrum experiences only minor changes with the time. The spectrum evidences no stimulated emission, which is expected to give a negative signal in the fluorescence band region. The transient absorption dominates over the stimulated emission. The stimulated emission is either very weak or relaxes more rapidly than our time resolution. The absence of the dynamics of the transient spectrum, which one could expect due to the decay of the stimulated emission, and also very weak fluorescence intensity imply that

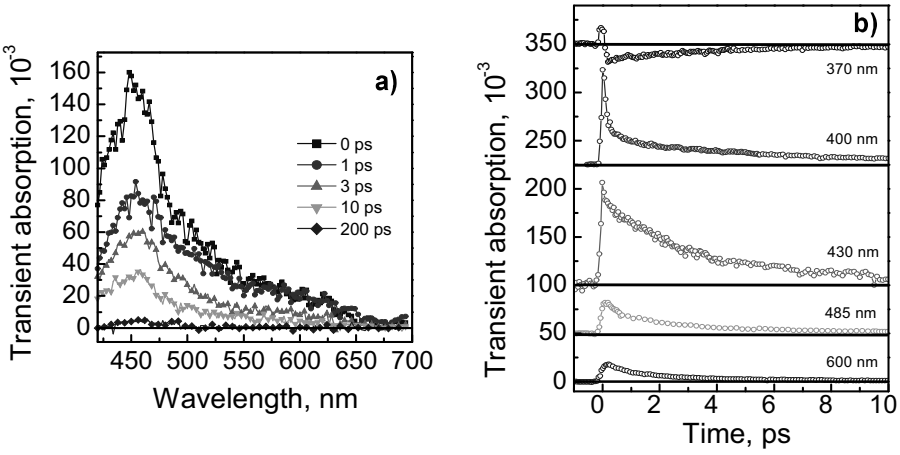

Fig. 4.3. Transient differential absorption spectra (a) and kinetics at various probe wavelength (b) of PPI-CAzPA dendrimer in DMSO solution, λ_{exc}= 350 nm.

the stimulated emission decays very rapidly, faster than the time resolution of our setum. The CAzPA chromophore groups evidently experiences very fast relaxation to the weakly emitting state.

Transient absorption kinetics gives more information about the relaxation process. The relaxation kinetics of the PPI-CAzPA dendrimer in DMSO solution measured at different probe wavelengths after the sample excitation with $\lambda = 350$ nm, i.e. to the π - π^* absorption band are presented in Fig. 4.3b. The short-lived induced absorption observed when the excitation and probe pulses overlap – shall be attributed to the two-photon absorption in DMSO solvent, as it was also observed in a pure DMSO. The decay kinetics at the different probe wavelengths are slightly different indicating that someevolution of the transient absorption spectrum does take place. Approximation of the kinetics at different wavelengths with a biexponential decay function gives a short relaxation time ranging between 2 and 3 ps and a weak component with the relaxationt im much longer than 1 ns. The transient absorption kinetics of the PPI and PAMAM dendrimers are identical within the experimental accuracy (see Fig. 4.4a). No evident differences in the transient absorption kinetics were also observed between PPI-CAzPA solutions in DMSO and in chloroform (Fig. 4.4 b). The kinetics was also insensitive to the excitation wavelength; no clear difference was observed between curves obtained with excitation to the π - π^* and n - π^* bands (Fig. 4.4c).

If we compare the transient absorption properties of the dendrimers and azobenzenes in hexane solution presented in Ref. [114, 131], we observe quiet close similarity and also some important differences. No stimulated emission was observed both in the dendrimers and in azobenzenes solutions. The excited state absorption decay in both cases took place on a time scale of several pc, and in both cases it was slightly faster at long wavelengths (see Fig. 4.3a). However, the shape of the excited state absorption spectrum and its evolution were significantly different. Clearly different shapes of the excited state absorption spectra were observed in azobenzenes solution at different delay times [114].

The relaxation process of azobenzene was interpreted as being determined by the excited state isomerization, and several isomerization phases and pathways were distinguished from the spectrum evolution and its dependence on the excitation photon energy [114, 131] [132]. The transient absorption evolution in dendrimers solution is less pronounced, therefore we cannot clearly distinguish relaxation phases and pathways. However, based on the similar excited-state relaxation rate we conclude that the excited-state relaxation of dendrimers in solutions is also determined by the excited state isomerization. Faster excited state absorption relaxation at long wavelengths, which in [114] was attributed to the relaxation via n - π^* state, indicates that the isomerization reaction occurs in a similar way as for azobenzenes. We relate the less pronounced spectra dynamics to the dendrimers influence. Probably nonuniform CAzPA group interaction with the dendrimers core causes distribution of isomerization rates and

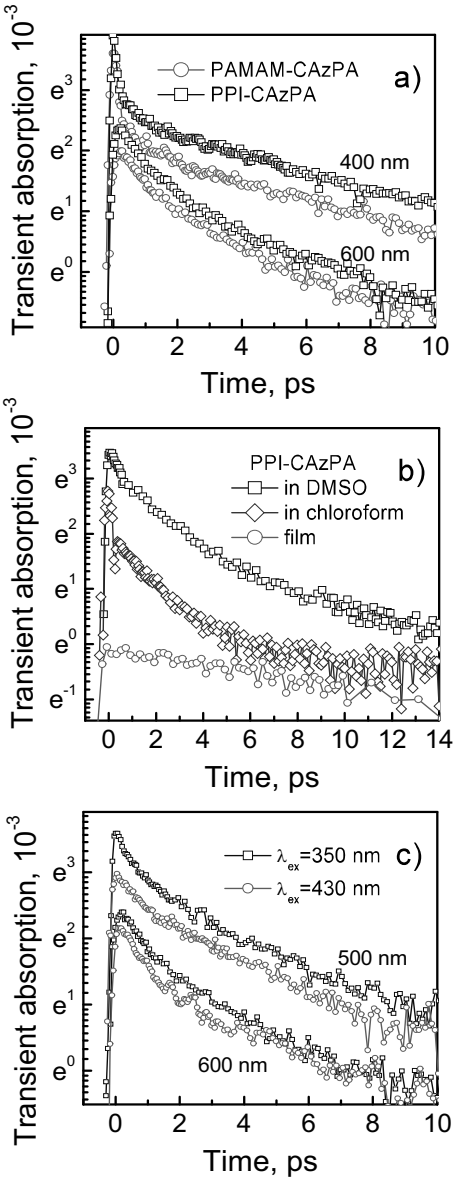

Fig. 4.4. a)Transient absorption kinetics of PPI-CAzPA and PAMAM-CAzPA in DMSO solution measured at 400 nm and 600 nm, λ_{exc}= 350 nm. (b) Transient absorption kinetics of PPI-CAzPA in different solvents and in film probed at 485 nm, λ_{exc}= 350 nm. (c) Transient absorption kinetics of PAMAM-CAzPA in DMSO solution at 500 nm and 600 nm measured with different excitation wavelengths.

consequently blurs the spectra evolution. Another reason may be the influence of the attached NO group and dendrimers branches, which influence the absorption and fluorescence spectra. However, we consider this reason as less probable because quiet clear transient absorption spectra dynamics was also observed in solution of substituted azobenzene [132], possessing even more modified absorption and fluorescence spectra in comparison with those of azobenzenes.

It should be noted that the observed excited-state relaxation is not a real isomerization reaction. Excited state twisting is a more correct term. The main majority of CAzPA groups relax back to the *trans* state. Conformational motions just favour very fast excited-state relaxation. The weak slow relaxation component should be related to the transfer of a small fraction of *trans* conformation molecules to the ground state *cis* conformation. Relaxation of the *cis* form back to the trans conformation evidently lasts much longer than our observation time of 1 ns.

We have also investigated the transient absorption in PPI-CAzPA dendrimers films. Fig. 4.4b shows the transient absorption kinetics taken at 485 nm. Relaxation kinetics at other probe wavelengths was very similar. The relaxation kinetics is close to exponential with the time constant of about 15 ps. In comparison with solutions the relaxation in the film is about 7 times slower. Taking into account very different viscosity of the dendrimers solid in comparison with the solvents used in this investigation the difference in relaxation rates is surprisingly small. Molecule motions in a solid state should be much more hindered if the isomerization reaction is controlled by the solvent viscosity. For example, relaxation of other type molecules (N,N-dimethylaninobenzylidine-1,3-indandione) in low viscosity solutions and embedded in polymeric matrix differs almost hundred times [174]. A similar differences was also observed in fluorescence yields. Similar isomerization rates of CAzPA fragment, occurs by combined action of two reaction pathways and involves only a relatively small amplitude motion of bulky molecule fragments. CAzPA molecules in a dendrimers solid have some free space, and

this space is evidently sufficient for the molecule motion during the isomerization reaction. Therefore, the isomerization reaction only slightly depends on the environmental viscosity.

4.3. Short summary

Femtosecond transient absorption investigations of PPI and PAMAM dendrimers functionalized with the azobenzene-type terminal groups revealed ultrafast excited-state relaxation taking place in solutions on a time scale of several picoseconds. Comparison of the relaxation properties with those of azobenzene molecules allows us to conclude that the ultrafast relaxation is caused by the excited state *trans–cis* isomerization. The conformational motions lead to the excited-state relaxation, and only a small fraction of molecules are transferred to the *cis* state. The isomerization rate is insensitive to the dendrimer core, solvent and excitation wavelength and is only about seven times slower in a solid dendrimer film. Similar isomerization rates of CAzPA groups in solution nand i solid film are interpreted in terms of a relatively small amplitude conformational motions taking place during the isomerization reaction.

5. Exciton migration and quenching in PPI-ESA dendrimers

In this chapter exciton relaxation and migration properties of the third generation PPI-ESA dendrimer in chloroform solution and in films are presented. We will show that the interchromophore interactions in dendrimers become important in a solid state and that it speeds up the exciton migration.

5.1. Dendrimers in chloroform solution

The structure of investigated third generation dendrimer is presented in Fig. 2.2. It posses an architecture consisting of a central dendrimer core (DAB), branched repeating units and exterior composed of terminal flexible chains, where ESA chromophore groups are attached.

The synthesis of PPI dendrimer [151] was carefully introduced in experimental section 2.1.2. The dendrimer solvents and films were prepared for optical absorption and fluorescence investigations as follows. The powder like dendrimers were dissolved in chloroform solution and investigated in 10 mm quartz cuvettes. The dendrimer concentration was about 2×10^{-5} mol/l and the optical density of the sample at 375 nm excitation wavelength was about 0.2. The dendrimer films were prepared by heating the dendrimer powder above the melting temperature (~60° C) and by pressing between two 20 mm of diameter quartz substrates with a 5-μm spacer.

The steady state spectroscopy and time resolved fluorescence were measured with the setup which was also described in detail in section 2.2. Only the some parameters of picosecond pulsed diode laser were chosen specifically for such experiment. The laser emitting 50 ps duration and 375 nm wavelength pulses at 20 MHz repetition rate was used for excitation. The average excitation power was about 150 mW/mm^2.

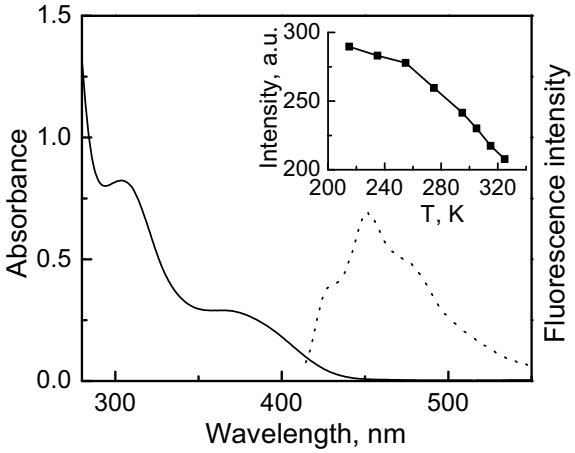

Fig. 5.1. Absorption and fluorescence spectra of the PPI dendrimer in chlorophorm solution. The insert shows the temperature dependence of the fluorescence intensity.

The typical steady state absorption and fluorescence spectra of the third generation PPI-ESA dendrimer in chloroform solution is shown in Fig. 5.1. The dendrimer extinction coefficient in the visible and near UV region is proportional to the chain number, therefore absorbance in this spectral region shall be attributed to the peripherally attached dendrimer chains. The fluorescence band in solution is shifted by about 4000 cm^{-1} to the low energy side relative to the lowest energy absorption band. The fluorescence spectrum shows a vibronic structure with about 1200 cm^{-1} spacing between vibrational components. By changing the temperature from 215 K to 325 K within the liquid phase range of chloroform solution, the fluorescence spectrum shifts to shorter wavelengths by about 4 nm and the fluorescence intensity integrated over the entire fluorescence band drops by about 30 %.

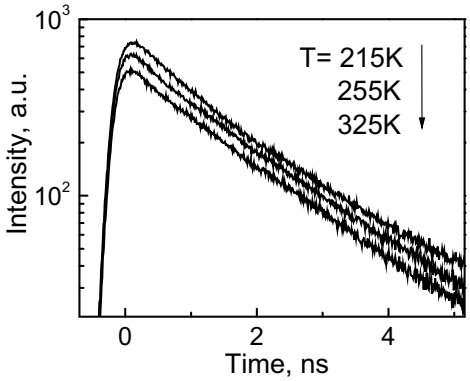

Fig. 5.2. Fluorescence relaxation kinetics of the third generation PPI-ESA dendrimer in chloroform solution measured at 450 nm at different temperatures.

The time-resolved fluorescence intensity decays almost exponentially with time constant of 1.54±0.1 ns (Fig. 5.2) and it's independent of the detection wavelength. The decay rate with experimental accuracy is also independent of temperature, only the initial fluorescence intensity slightly drops with temperature and causes some weakening of the time-integrated fluorescence. The fluorescence weakening is evidently caused by changes in the sample absorbance rather than by fluorescence properties. Solvent expansion, which causes about 15 % decrease in the dendrimer density within the investigated temperature range, is responsible for about 15 % drop of the fluorescence intensity. Additional absorbance variation is evidently caused by modification of the dendrimer absorption spectrum. The temperature independent fluorescence relaxation rate shows that both radiative and nonradiative excited state relaxation rates are independent or only weakly dependent on temperature.

The fluorescence Stokes shift evidently appears faster than during about 100 ps time resolution of our setup. We can conclude that the Stokes shift is caused by excited state vibrational relaxation and salvation, which in low viscosity solvents usually terminate during several picoseconds. The intradendrimer energy migration between chromophore moieties, which, as we will slow later, is much slower, evidently has no influence on the fluorescence spectrum and decay kinetics.

In order to determine the intradendrimer energy migration rate, we have measured the fluorescence depolarization dynamics. The insert in Fig. 5.3 shows the fluorescence kinetics measured at parallel (I_{II}) and perpendicular ($I_{\perp}$) excitation and detection polarizations at room temperature. Fig. 5.3 shows anisotropy decay kinetics at different temperatures determined as:

$$r = \frac{I_{\parallel} - I_{\perp}}{I_{\parallel} + 2I_{\perp}} \tag{5.1}$$

Anisotropy decays single exponentially with the experimental errors, and the decay is faster at higher temperatures.

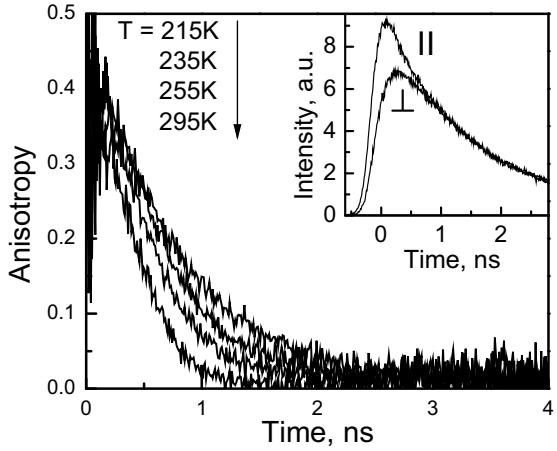

Fig. 5.3. Fluorescence anisotropy kinetics of the PPI-[C2] 16 dendrimers in chloroform solution at different temperatures. The insert shows the fluorescence kinetics at 450 nm for parallel and perpendicular excitation and detection polarization measured at 295 K which were used to calculate the anisotropy kinetics.

Fig. 5.4 shows the temperature dependence of anisotropy decay time. In addition to the intradendrimer excitation energy migration, rotation diffusion of the entire dendrimer and reorientation of the chromophore units may also contribute to the anisotropy decay kinetics. We will analyze which of the processes determines the anisotropy kinetics. The dendrimer rotational correlation time may be estimated from the Stokes-Einstein relation $\Theta = (\eta V)/(RT)$, where η is the solvent viscosity, V is dendrimer volume, T is the temperature and R is the ideal gas constant. The temperature dependence of the G3 PPI-ESA dendrimer fluorescence depolarization time is in good agreement with the Stokes-Einstein relation. It is quiet well presented in Fig. 5.4 where theoretical dependence is normalized to the

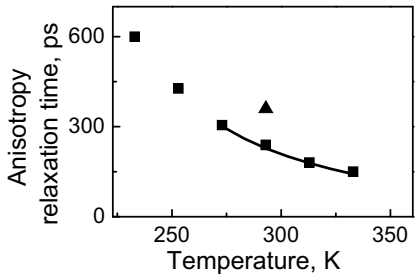

Fig. 5.4. Temperature dependence of the fluorescence anisotropy relaxation time of PPI-[C2] 16 dendrimer in chloroform solution (squares). The triangle shows the anisotropy relaxation time of the fourth generation-dendrimer with 32 functional groups.

experimental data. Exact calculation of the correlation time is difficult because it is quiet difficult to determine volume of dendrimer. Due to the chain folding the effective dendrimer volume is evidently significantly smaller than that of idealized ball like structure with radius determined by the chain length, but larger than that of the densely packed molecular structure with the atom number equal to that of the dendrimer. Calculation of the two limiting cases allows the estimation of the rotational correlation which is of the order of several nanoseconds. Similar values may also be obtained from the comparison with the known rotational correlation times of another similar-sized molecules. Thus, rotational diffusion of the entire dendrimer is evidently too slow to cause of the experimentally observed fluorescence depolarization rate. Flexible dendrimer branches evidently allow significant freedom of the chromophore motion and may also cause fluorescence depolarization. By comparing the chromophore size with sizes of different molecules with the available information about their reorientation times we conclude that the chromophore reorientation may take place on a subnanosecond time scale. We have also measured the fluorescence anisotropy relaxation time of the fourth generation dendrimer with the two times larger chromophore number. At room temperature it shows about 1.5 times longer depolarization time than the third generation dendrimer. The fourth generation dendrimer has about 13 % larger radius and about 30 % larger surface area. Two times larger number of chromophore units are consequently about 1.5 times more densely packed. The average interchromophore distance are about 1.2 times shorter. Taking into account the $1/R^6$ energy transfer rate dependence, where R is an interchromophore distance, the energy transfer, and, thus the fluorescence depolarization rate shall be about three times faster in the fourth-generation dendrimer. Since this is not the case the energy transfer is evidently not the main depolarization factor. The slower fluorescence depolarization of the larger dendrimer shall be attributed to the denser chromophore packing where they have less freedom for the reorientational motion. Thus, based on several experimental evidences, we conclude that the fluorescence anisotropy

relaxation is mainly caused by the chromophore reorientation. The energy migration inside the third generation dendrimer is evidently slower and plays no dominant role. The interchromophore exciton transfer time, thus, is evidently significantly longer than the 150-600 ps fluorescence anisotropy relaxation time. This conclusion is in contrast with the strong interchromophore coupling observed in some dendrimers, for instance in PPI functionalized with oligo(*p*-phenylenevinylene) [175]. Properties of functional groups, their transition dipole moments, size, and flexibility evidently determine the interchromophore coupling, rather than the dendritic structure. Low extinction coefficient of the G3 PPI-ESA dendrimer chromophore groups, which is only about 1000 $M^{-1}cm^{-1}$ at the maximum of lowest energy absorption band, and weak absorption and fluorescence band overlap are evidently responsible for the weak interchromophore coupling and slow energy migration.

5.2. Dendrimer film

Fig. 5.5 shows fluorescence, fluorescence excitation spectra and long wavelength edge of the absorption spectrum of the G3 PPI-ESA dendrimer film at room temperature. The fluorescence band is shifted to the long

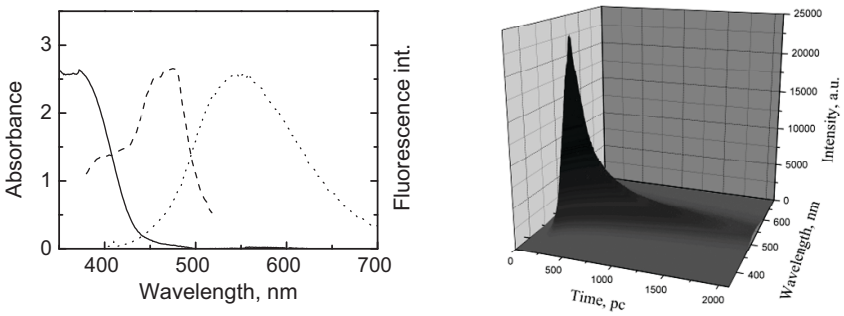

Fig. 5.5. a) Absorption (solid line), fluorescence (dot line) and fluorescence excitation (dash line) spectra. b) images of fluorescence intensity as a function of time and wavelength. Neasurements performed for the dendrimer films at the room temperature.

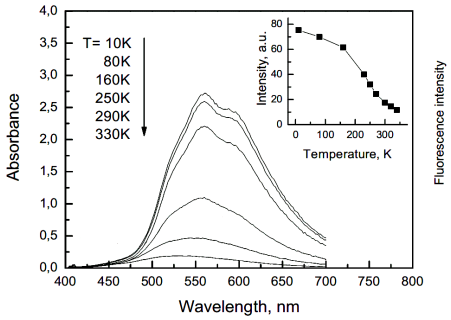

Fig. 5.6. Fluorescence spectra of the dendrimer film at different temperatures. The insert shows the temperature dependence of the fluorescence intensity integrated over the fluorescence band.

wavelength region by about 100 nm with respect to the solution fluorescence band. So a large shift can hardly be related to solvent effects. Strong modification of the absorption and fluorescence spectra is typical of molecular solids because of the formation of collective excitonic states. Dendrimer branches are squeezed and/or chromophores from different dendrimers appears close to each other and the excitonic interaction evidently results in formation of collective states. Because of the large optical density of the available films, the absorption spectrum measurement was possible only at the long wavelength tail of the absorption band. Despite an apparent difference, normalization of the absorption spectra of the film and solution shows that they are very similar. Thus, the collective states, which we attributed to the film fluorescence, are not observable in the film absorption. Their concentration is evidently very low, but due to the effective excitation energy transfer they dominate in the fluorescence spectrum.

In contrast to solution, dendrimer films show strong temperature dependence of the fluorescence spectrum. This dependence is presented in Fig. 5.6. The fluorescence intensity of the dendrimer film decreases more than six times, when the sample is heated from 10 K to 340 K (insert in Fig. 5.6). The film fluorescence

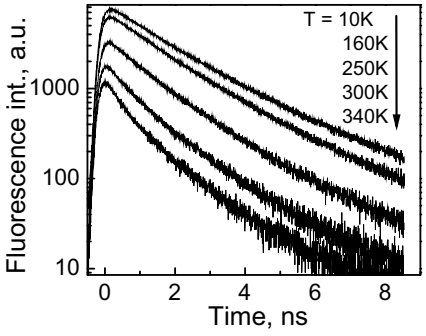

Fig. 5.7. Fluorescence decay kinetics of the dendrimer film measured at 550 nm at different temperatures.

decrease in the 223-320 K range is about four times stronger than in the case of solution. Fig. 5.7 shows the temperature dependence of the fluorescence decay kinetics measured at the maximum of the fluorescence band. The initial fluorescence intensity decreases and it's relaxation becomes faster with an increase in the temperature. Assuming that fluorescence intensity is proportional to the exciton density, we can express the exciton kinetics as:

$$\frac{dn}{dt} = -k(t)n \qquad (5.2)$$

where n is density of excitons and $k(t)$ is the time dependent relaxation rate. We can determine the time dependence of the exciton decay rate from fluorescence decays by using Eq. (5.2). Direct differentiation of the fluorescence kinetics gives very large errors. Therefore the kinetics were approximated by multiexponential functions, simulatenously performing deconvolution of the apparatus function, and was differentiated afterwards. Fig. 5.8 shows the obtained time dependences of the excitation decay rate. At the low temperatures of up to 160 K the excitation decay rate decreases only slightly during the initial several nanoseconds. We attribute the time dependence of the decay rate to the inhomogenity of the system, or to the presence of some exciton quenching centers. At higher temperatures a fast decay rate component with about 120 ps time constant appears and its relative contribution increases with temperature. The strong temperature dependence indicates that some temperature-activated process is responsible for the decay. Excitons migration in the heterogenous system and their quenching by some quenching centers existing in the dendrimer material is the most probable exciton decay mechanism. The quenching centers may be formed by the chemical impurities or by

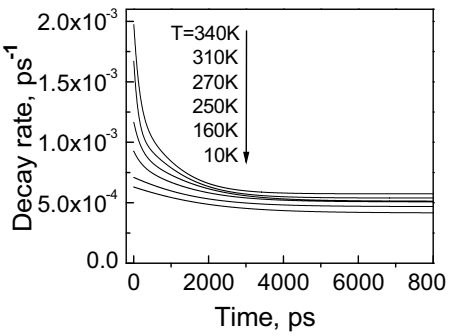

Fig. 5.8. Time dependence of the fluorescence relaxation rate of the dendrimer film at different temperatures.

photooxidized dendrimer fragments. Excitons reach the quenching centers during the migration process or by direct energy transfer. Later, we will demonstrate that in contrast to the isolated dendrimer in solution the exciton migration in the film plays an important role. Temperature activated exciton migration evidently takes place during the initial several hundreds of picoseconds until they are trapped in deep traps.

The fluorescence spectrum of the dendrimer film shows a clear evolution with time. Fig. 5.9 presents the time-resolved fluorescence spectra at different times after excitation constructed from the fluorescence kinetics obtained at room temperature. The insert in Fig. 5.9 shows the shift dynamics of the fluorescence band maximum. The time-resolved fluorescence band shift shall be attributed to the spectral diffusion observed in many disordered systems such as conjugated [176-178] and nonconjugated polymers [179], amorphous molecular glasses [180] and orientationally disordered molecular crystals [181] [182]. The temperature dependence of the shift dynamics is weak. It slightly slows down at low temperatures. This bahaviour is in agreement with the calculations performed in [179], where the authors show that the temperature dependence of the spectral diffusion appears only on the long time scale, while the initial relaxation part is temperature independent.

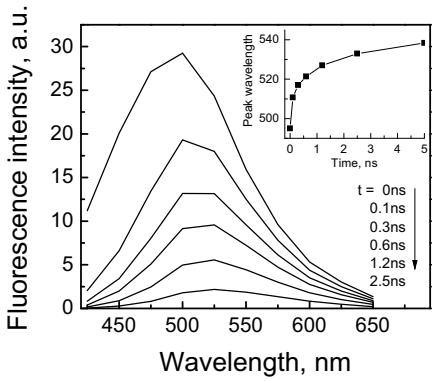

Fig. 5.9. Time-resolved fluorescence spectra of the dendrimer film at room temperature. The spectra were constructed from the fluorescence decay kinetics. The insert shows the shift dynamics of the fluorescence band maximum.

Fig. 5.10 shows the fluorescence kinetics of the dendrimer film at parallel and perpendicular excitation and detection polarizations measured at room temperature at different probe wavelengths. The insert shows the calculated anisotropy kinetics. The low anisotropy values indicate that the main part of the fluorescence depolarization takes place faster than the time

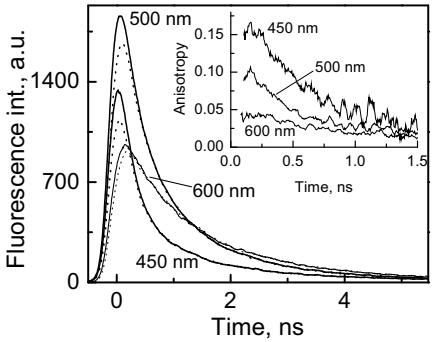

Fig. 5.10. Fluorescence kinetics of the dendrimer film at room temperature measured at different detection wavelengths at parallel(solid lines) and perpendicular (dashed lines) excitation and detection polarizations. The insert shows the fluorescence anisotropy kinetics at .different wavelengths calculated from related decay kinetics.

resolution of our setup. Dendrimers and their chromophores have little reorientation freedom in a solid state, thus can hardly cause so fast fluorescence depolarization. Hence fluorescence depolarization shall be attributed to the exciton diffusion. The largest anisotropy was determined at 450 nm detection, whereas at 600 nm the anisotropy decays slightly slower. These properties are in agreement with the exciton diffusion. The slow anisotropy part evidently originates from the excitons already trapped at low energy sites. Low anisotropy values observed at long probe wavelengths indicate that the excitons radiating at long wavelengths are not created directly by the light absorption, but are transferred from high erenergy sites, causing fluorescence depolarization. Excitons located at low energy sites are less mobile, therefore fluorescence anisotropy at long wavelengths decays slightly slower. The fluorescence anisotropy values and decay kinetics within experimental accuracy are independent of the temperature. This observation is in agreement with the transient absorption depolarization data obtained for conjugated MEH-PPV polymer, where only weak temperature dependence of the depolarization kinetics was observed [183]. This feature correlates well with the weak temperature dependence of the fluorescence band shift kinetics and shows that the fluorescence depolarization is related to the energetically downward excitation hopping, which dominates during the initial times.

The final anisotropy depolarization rate is by about two orders of magnitude slower than it was observed, for example, in conjugated polymers where it took place on a time scale of tens of picoseconds [183, 184]. We can

estimate the interchromophore exciton hopping time knowing that in conjugated polymers it is of the order of hundreds of fs [183, 184, 185]. Two orders of magnitude slower depolarization suggests that the interchromophore hopping time in third generation dendrimers is of the order of tens of picoseconds.

5.3. Interpretation of the results

Fluorescence properties of the third generation PPI-ESA dendrimer solid films are typical of amorphous molecular solids. We observe no evidences, which could be attributed to a specific dendrimer structure. Close dendrimers packing evidently cleans the difference between intradendrimer and interdendrimer chromophore interactions.

As we have already discussed, the nonexponential fluorescence decay, fluorescence band shift and fluorescence anisotropy decay show different temperature dependences, although we relate all of them to the exciton migration. However, they reflect slightly different processes. The fluorescence band shift and depolarization are related to the energy migration within the host chromophore molecules, while the fluorescence quenching is related to the energy transfer to quenching centers. The fluorescence band shift reflects the energetically downward excitation hopping. Other two processes are caused by all downward, isoenergetical and thermally activated upward jumps. In case of energy quenching in disordered systems the exciton relaxation kinetics may be expressed as [182]:

$$\frac{dn}{dt} = -kn - q\nu_0^{\alpha} t^{\alpha-1} n \tag{5.3}$$

where q is the quencher concentration, ν_0 is the quenching rate and α is the parameter determining the quenching time dependence. In three-dimensional system this parameter depends on the dispersion σ of Gaussian distribution of energy of states and temperature as [182]:

$$\alpha = \frac{1}{1+\left(\frac{\sigma}{4kT}\right)^2} \tag{5.4}$$

This parameter equals one in the limits of diffusion-limitted exciton migration, i.e. when the energy disorder is low in comparison with kT and, thus, excitons are not trapped. The exciton quenching rate in this case is time independent and the exciton concentration decays exponentially. In the opposite case when the energetical disorder is large in comparison with kT the exciton quenching takes place without exciton migration by the static direct energy transfer trom the excited chromophore molecule to the quencher. Because of distributed excited chromophore-quencher distances the quenching rate decreases with time. Thus, this theory predicts a time-independent exciton relaxation rate at high temperatures which decreases with time at low temperatures. We observe a relaxation rate that decreases with time in the whole 10-340 K temperature range. We attribute the long time relaxation rate to the intrinsic excitation relaxation. The intrinsic relaxation time varies from 1.8 ns at room temperature to 2.4 ns at 10 K. At room temperature the intrinsic relaxation time is very close to that of 1.53 ns for the dendrimer solution. The time-dependent relaxation rate part at low temperatures shall be attributed to the exciton quenching due to the steric energy transfer or/and due to the excitons migration during their localization to the bottom of the distribution of the density of states. At about 160 K, the thermal energy evidently becomes comparable to the energy disorder, i.e. $\sigma \approx 4\,kT$, and the relaxation rate starts to grow. At 340 K the energy disorder still remains comparable with kT and we still observe the time-dependent relaxation rate. The fluorescence excitation spectrum confirms a large energy disorder. It shows that the maximal fluorescence efficiency may be achieved under the sample excitation to the absorption band tail, i.e. to the tail of the density of states. Evidently excitons created under these excitation conditions are less mobile and have lower probability of being quenched. Other effect such as inhomogenity of sample may also make the time dependence of the relaxation rate more pronounced.

The quencher concentration may be larger near the layer surface due to the impurities absorbed from the ambient air, oxidized chromophores or other dendrimer parts. In this case the excitons decay rate may be different depending on their distance from the layer surface. This would lead to the nonexponential exciton decay even when the decay rate in some particular sample position is time independent. It should be noted that the fluorescence excitation spectrum may also be influenced by this effect. Because of the large optical density of the sample at short excitation wavelengths the light is absorbed in a thin sample layer near the surface. The estimation based on comparison of the film and solution absorption spectra shows that the light is absorbed in a layer of several hundred nanometers under the 375 nm excitation.

5.4. Short summary

Exciton migration and quenching process in a single dendrimer in solution and in a solid state dendrimer film are significantly different. No signatures of the exciton quenching and migration in dendrimer solution were observed. Insteed the fluorescence depolarization is determined by the chromophore reorientation with time constant ranging from about 150 ps at 333 K to 600 ps at 233 K, while the exciton migration is much slower. Colective excitation states are formed in a solid state, which cause the long wavelength schift of the dendrimer fluorescence band. The exciton relaxation rate in a dendrimer solid film is strongly enchanced by the exciton quenching, which is particularly rapid at high temperatures. The temperature and time dependence of the quenching rate indicate a wide, in comparison with thermal energy, distribution of the exciton state energies. The fluorescence depolarization in solid state, which is caused by the exciton migration, takes place on a subnanosecond – nanosecond time scale and indicates that the interchromophore energy transfer time is of the order of tens of picoseconds.

6. Tautomeric forms and excited state dynamics of PPI dendrimers functionalized with ESA chromophores

Here we present investigations of the poly(propylene-imine) (PPI) dendrimers functionalized with 4-(4′-ethoxybenzoyloxy)salicylaldehyde chromophore moiety (PPI-ESA). Terminating groups attached to the core chains form salicylidenimine functional groups, which, as it was already mentioned, determine the near UV absorption and fluorescence properties of the dendrimers. Keto-enol tautomerization of the salicylidenimine functional group may take place due to intramolecular proton shifts between the phenol–oxygen and the imine–nitrogen, via intramolecular hydrogen bonding O–H···N or O···H–N determining their excited state dynamics. Potential possibility to change tautomeric form of functional groups by their excitation suggest a simple way to control functional properties of dendrimes by light, what may open already mentioned application possibilities.

In this chapter we report ultrafast transient absorption investigations of the first (G1) and fifth (G5) generation PPI-ESA dendrimers in solutions combined with the quantum chemistry calculations of their electronic and conformational structure. Our investigations show that the dominating tautomeric form of dendrimer terminating groups depends on the dendrimer generation. Different tautomeric forms are dominantly excited by different wavelength excitation light and experience different ultrafast excited state dynamics.

6.1. Steady state absorption and QC calculations

Fig. 6.1a shows steady state absorption and fluorescence excitation spectra of the investigated dendrimers (G1 and G5) in chloroform solution. Optical absorption spectra have several distinct absorption bands. The high-intensity absorption band at about 305 nm is similar for dendrimers of both generations. However, longer wavelength band peaks at 400 nm and 375 nm for G1 and G5 dendrimers, respectively, and has much higher intensity for the G5 dendrimer.

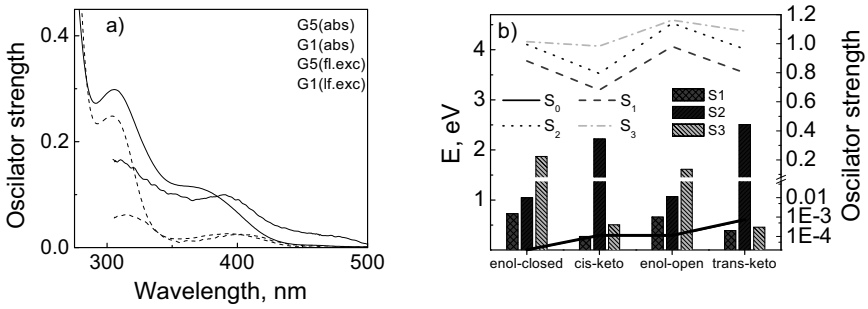

Fig. 6.1. a) Absorption and fluorescence excitation spectra of the first (dots) and the fifth (lines) generation dendrimers. b) The ground and three lowest excited singlet state energies (lines), and oscillator strengths (columns) of the optical transitions of the dendrimer chromophore in different tautomeric forms calculated in vacuum.

G5 also has a weak absorption tail stretching to 500 nm. Quantum chemistry calculations have been also performed in order to interpret the absorption spectra. Calculation results for the isolated molecules in vacuum indicate that functional groups of dendrimers could be found in the four most stabile tautomeric forms, which are presented in Fig. 6.2. Total energies of terminating groups in the ground state geometries optimized by using HF/6-311G(d,p) and HF/6-311G(2df,2pd) basis sets have been calculated for different tautomeric forms in the electronic ground state and three lowest energy excited states, as well as oscillator strengths of corresponding optical transitions. Figure 6.1b presents the calculation results.

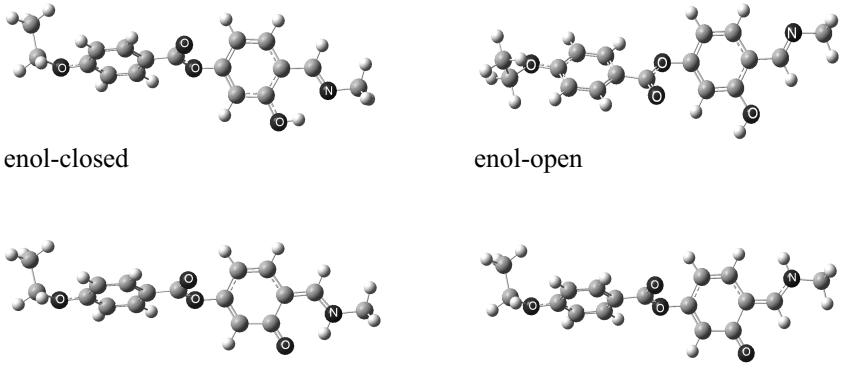

enol-closed enol-open

cis-keto (closed) *trans*-keto (open)

Fig. 6.2. Calculated structures of the four most stabile tautomeric forms of dendrimer terminating groups.

As an example, Fig. 6.3 also shows distributions of electronic wave functions in the ground and excited states of various enol-closed tautomers.

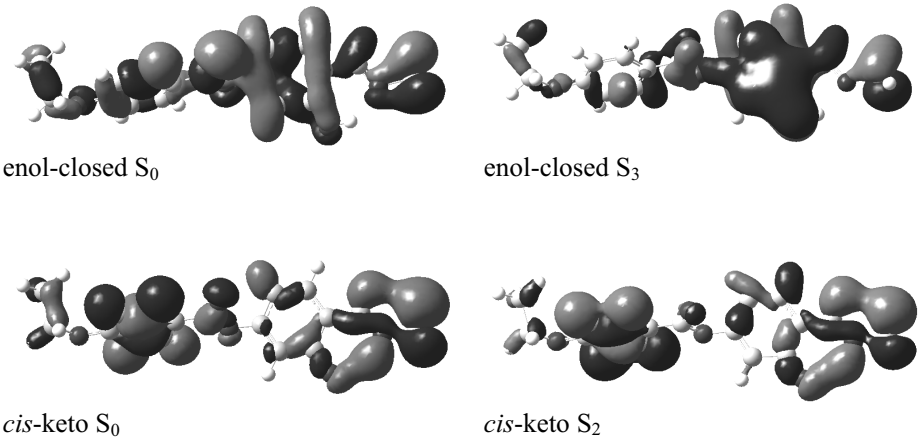

Fig. 6.3. Electron densities of several enol-keto tautomeric forms of dendrimer terminating groups in ground and in excited states.

Terminating groups in an enol-closed tautomeric form, i.e. possessing hydroxyl group and a Schiff base in a closed cycle completed by a hydrogen bond, have the lowest energy in a ground state. The *cis*-keto tautomer with the protonated Schiff base has energy higher by about 250 meV, than enol-closed tautomer. Open isomers have about 250 meV higher energies both in enol and keto forms than closed isomers. This difference is evidently caused by the formation of the hydrogen bond in the closed form of molecules. The optical transition energies and oscillator strengths are presented in Fig. 6.1b for comparison with the experimental absorption spectra. According to the calculations, the enol-closed tautomers have strong electronic transition at 298 nm, which is in a good agreement with the experimentally observed strong absorption band at about 305 nm. Equivalent electronic transition of the enol-open tautomers has slightly higher energy. *Cis*-keto and *trans*-keto tautomers have strong electronic transitions at 384 and 363 nm respectively, which are also in a good agreement with the absorption band positions of dendrimer solutions. Therefore, absorption bands in the 350 – 400 nm region shall be attributed to the keto tautomeric form. Optical transitions to the lowest energy

electronic states have very weak oscillator strengths for all the tautomeric forms. Estimation of the ratio of relative concentrations of terminating groups in different tautomeric forms from the absorption band intensities, taking into account about two-fold larger oscillator strength of the keto tautomers (Fig. 6.1b), gives that about 5% and 20% of terminating groups are in keto form in G1 and G5 dendrimers respectively. Such relatively high keto tautomer concentration is in apparent disagreement with the large, about 10 kT (~250meV), energy difference between the enol and keto form tautomers in the ground state. Probability of the keto form formation shall be negligible. However, it shall be noted that the calculations were performed for the isolated molecules, not accounting for the solvent influence. It is well known, that solvents strongly influence the keto-enol tautomerization [186]. The influence is particularly strong in case of protic solvents, which form hydrogen bonds with N and O atoms. Although chlorophorm is aprotic solvent, small amount of water molecules could be adsorbed from air.

The difference between absorption spectra of G1 and G5 dendrimers is more intriguing question. Both dendrimers have identical terminating groups, which are bound to identical dendrimer chains, therefore absorption spectra are expected to be also identical. The only influence may come from interaction of terminating groups with other terminating groups or dendrimer chains. Two types of the influence of the interaction on the absorption properties may be anticipated: excitonic interaction between terminating groups and steric interaction influencing conformational states of terminating groups. Excitonic interaction caused by formation of dimmers or even larger aggregates may lead to the shifts of absorption bands or formation of new absorption bands. Thus, the long wavelength bands in such a case may be attributed to dimmers. However, the excitonic interaction shall be enormously strong to cause shift of the electronic transition by almost 1 eV. Moreover, close agreement between absorption band positions and calculation results suggests attribution of the long wavelength bands to the keto form. Interaction impact on the conformational states seems to be more plausible and may be related with the

formation of hydrogen between the separate ESA chromophores. Hydrogen bonds between separate chromophore groups in dendrimer molecule may influence its ground state energy. G5 dendrimers have 64 chains and large number of terminating groups that increases their interaction probability and H-formation possibility. They also evidently enhance the possibility of formation of higher energy tautomeric states, probably of open configuration. The presence of open form molecules in G5 dendrimers is in a good agreement with the calculation data. According to the calculation results the open keto form terminating groups (*trans*-keto) have strong optical transition at 363 nm, which is in a perfect agreement with the absorption band position of the G5 dendrimers. In case of G1 dendrimers, where such interactions are much less probable, terminating groups freely relax to the lower energy closed configuration. Closed keto tautomers (*cis*-keto) have absorption band at longer wavelength in agreement with the experimental data. Such attribution is also supported by the transient absorption data (see below).

Similar steady state absorption spectra have been observed for other molecules containing Schiff bases, where optical properties were also related to the presence of the *enol* and *keto* tautomeric forms [139, 187, 188]. Nevertheless, direct comparison of the absorption spectra is difficult, because electronic wave functions of the chromophoric groups both in the ground and excited states are delocalized over the entire terminating groups (see Fig. 6.3) indicating that structures of the entire terminating groups plays an important role in formation of their optical properties.

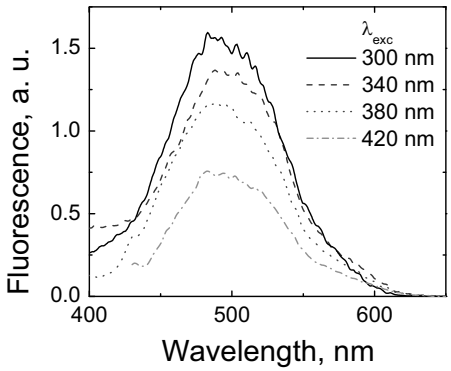

Fig. 6.4 Fluorescence spectra of G5 PPI-ESA dendrimer measured after excitation with different wavelengths

Figure 6.1a also shows the fluorescence excitation spectra

measured by detecting fluorescence at 530 nm. The excitation spectra reveal the same absorption bands as the absorption spectra, but their positions and relative intensities are slightly different. In the long wavelength region, excitation spectra of both dendrimers closely resemble the absorption band of G1 related to the *cis*-keto tautomeric form. Comparison of the absorption and the fluorescence excitation spectra shows that the lower energy bands are stronger expressed in the excitation spectra, indicating that species having lower energy electronic transitions have higher fluorescence yields. Therefore, the fluorescence quantum yield of G1 dendrimers is about 4 times lower under their excitation to the enol tautomer absorption band than under excitation to the keto tautomer absorption band. It should be also noted, that the fluorescence spectra show only very small differences under excitation at different wavelengths indicating that the fluorescence originates from the same molecular species independently of what molecular species have been excited. Fig. 6.4 shows fluorescence spectra of G5 dendrimer excited at different wavelengths. Tautomeric changes evidently take place in the excited state, as it has been demonstrated for other molecules with salicylidenimine functional group [188]. Fluorescence spectrum of our dendrimers is very similar to those of different Schiff base compounds where it generally has been attributed to the *cis*-keto tautomeric form [189]. Thus, dendrimer fluorescence shall be also attributed to some molecular excited state originating from the excited keto tautomers. The difference in intensities of absorption bands revealed by absorption and excitation spectra reflect different yields of fluorescence states obtained under excitation of different tautomeric species. The very small differences of the fluorescence spectrum shall be attributed to slightly different conformations of molecules causing inhomogeneous broadening of absorption bands, rather than to different tautomeric species. Excitation spectrum of the G5 dendrimer shows also the long wavelength band stretching up to 500 nm where weak absorption was also detected. Since this band is not observable in G1 dendrimer solution we also attribute it to some conformationaly distorted terminating groups. Strong manifestation of this band in fluorescence

excitation spectrum implies that these molecules possess higher fluorescence yield than other molecular species. According to the quantum chemical calculations, terminating groups in the keto form possesses a low energy n-π^* electronic transition at about 425 nm. This transition has very low oscillator strength (see Figure 6.1), however, according to the calculation results, it slightly increases upon conformational distortion of terminating groups. Thus, the dendrimer fluorescence probably originates form n-π^* states of keto tautomers.

6.2. Transient absorption

The presence of four different molecular species is additionally supported by the transient absorption data. Figures 6.4 - 6.7 show transient absorption spectra at different delay times and decay kinetics obtained for G1 and G5 dendrimer solutions after their excitation at 375 and 350 nm. According to the above discussion, the *cis*-keto tautomers dominantly absorb at 375 nm in G1 dendrimers, thus the transient absorption changes of G1 dendrimer excited at 375 nm shall be attributed to the *cis*-keto tautomers**.** At short delay times, the spectra show a negative transient absorption, which quite closely resembles the fluorescence spectrum of the dendrimers, thus, it shall unambiguously be attributed to the stimulated emission. An induced absorption is observed at longer wavelengths. The induced absorption decays almost simultaneously with the stimulated emission on tens of ps time scale, therefore it shall be attributed to the excited state absorption.

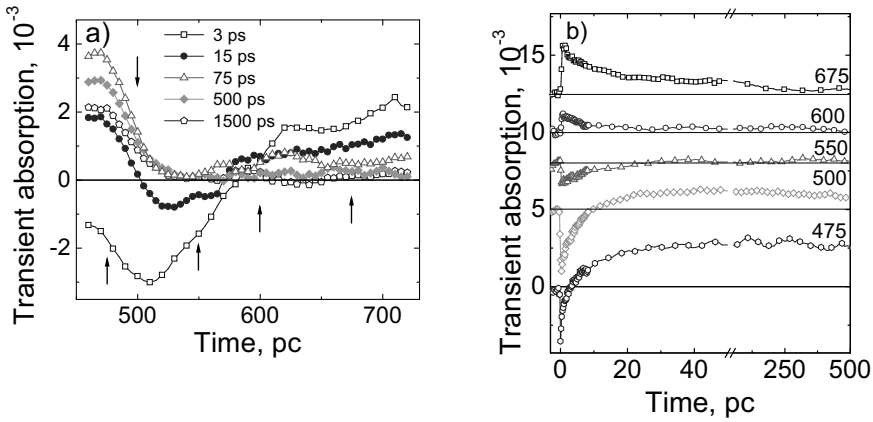

Fig. 6.4. Transient absorption spectra (a) and kinetics (b) of G1 PPI dendrimer measured with excitation at 375 nm.

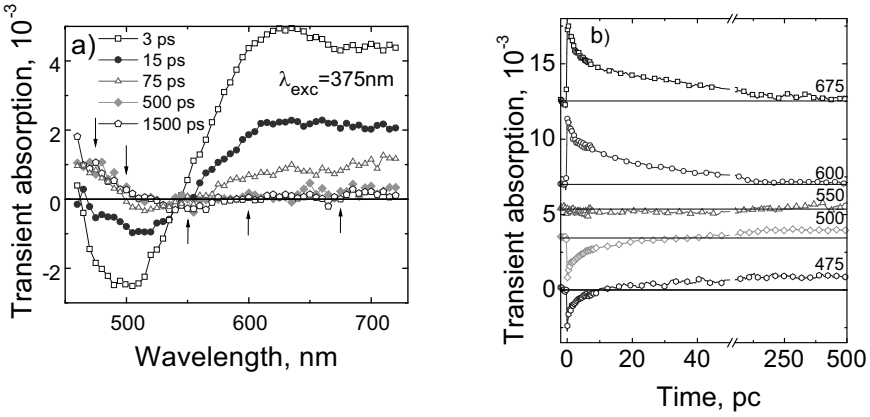

Fig. 6.5. Transient absorption spectra (a) and decay kinetics (b) of G5 PPI dendrimer measured with excitation at 375 nm.

A new induced absorption band emerges below 500 nm at longer delay times. This induced absorption band has long relaxation time, much longer than the 2 ns time interval of our measurements. The very long life time, gradual appearance, and the fact that the induced absorption appears in the same spectral region where the weak absorption band, attributed to the conformationaly distorted keto tautomers is present in G5 dendrimer solution, allow us to attribute it to the ground state molecules rather than to the excited state. Excited molecules evidently experience conformational changes and

relax to the ground state in the altered conformation. Transient absorption kinetics of G1 dendrimers reveals dynamics of the photoinduced processes. The kinetics in the 475-550 nm region is determined by the competition between the stimulated emission and the long living induced absorption. The stimulated emission at 475 nm appears instantaneously, rapidly decays, and turns into the induced absorption on a subpicosecond time scale. The rapid decay observed on the short wavelength side of the fluorescence band evidently reflects vibronic/conformational relaxation of excited molecules causing the rapid red shift of the stimulated emission band. The slower decay on a tens of ps time scale takes place simultaneously with the dominant decay of the induced absorption, thus reflects relaxation of terminating groups to the electronic ground state and formation of the conformationaly distorted ground state terminating groups. Based on comparison of the intensity of the long living induced absorption with the stimulated emission and excited state absorption we conclude that majority of G1 excited molecules are converted into the long living conformational isomers.

The induced absorption at long wavelengths (>550 nm) is evidently not affected by the absorption of the photoproduct, therefore we assume that its kinetics correctly reflects the excited state relaxation. The kinetics in this spectral region may be fitted with approximately 7 ps, 30 ps and 2000 ps decay time constants. This is consistent with the fluorescence relaxation with about 2 ns time constant and also revealing some fast initial decay component not resolved by the fluorescence spectrometer. This confirms attribution of the dominating dendrimer fluorescence to some molecular species, which are formed in a course of the excited state relaxation with a yield depending on the ground state species that were excited.

Transient absorption spectra of G5 dendrimers obtained with 375 nm excitation (Fig. 6.5a) are slightly different from those of G1. This dendrimer has additional absorption band at about 375 nm, which we attribute to *trans*-keto tautomers. It has broader absorption band of enol-tautomers therefore *trans*-keto and enol-closed tautomers may be also excited in addition to *cis*-

keto tautomers. The additional excited species cause a strong absorption band at about 630 nm, which was absent or very weak in G1 solution. This absorption band evidently stretches to the stimulated emission region and overcomes the long wavelength side of the stimulated emission band. The short wavelength part of the stimulated emission band is relatively weak in comparison with the induced absorption, which shows that the additional excited species do not contribute to the stimulated emission. The short wavelength induced absorption band is also relatively weak, thus the additional excited species evidently do not create the long living photoproduct states. The relaxation kinetics presented in Figure 6.5b shows an additional fast relaxation component in the induced absorption relaxation that shall be also attributed to the additional excited species.

In order to get more information which species cause additional transient absorption properties of G5 dendrimers we performed transient absorption investigations with different excitation wavelength. Figures 6.6-6.7 shows differential absorption spectra and decay kinetics of both dendrimers obtained under the excitation at 350 nm. The spectra of both dendrimers are significantly different from those obtained with 375 nm excitation. They show no stimulated emission in the fluorescence band region, and an induced absorption spectrum is clearly dominated by the band at 630 nm. This band is particularly strong in solution of G5 dendrimers. According to the transient absorption kinetics presented in both figures the induced absorption band at about 630 has a fast relaxation component of several ps in addition to the tens of ps relaxation observed under 375 nm excitation. Since both enol and keto tautomeric forms are evidently excited at 350 nm, the induced absorption band at 630 nm, which gains intensity under the short wavelength excitation, shall be attributed to the enol tautomers.

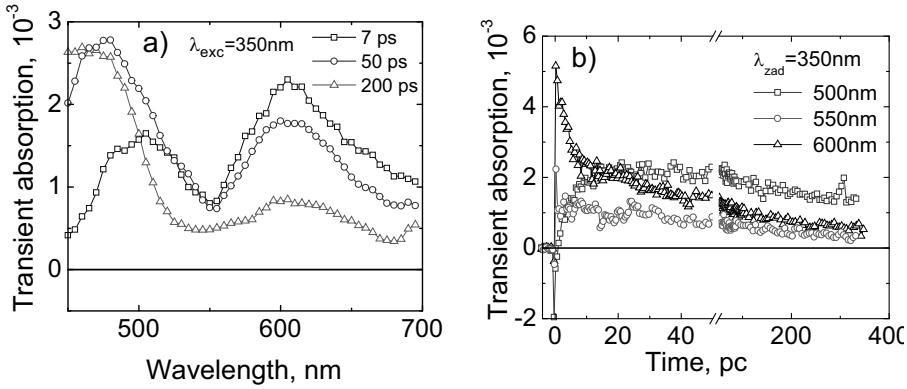

Fig. 6.6. Transient absorption spectra (a) and decay kinetics (b) of G1 PPI dendrimer measured with excitation at 350 nm.

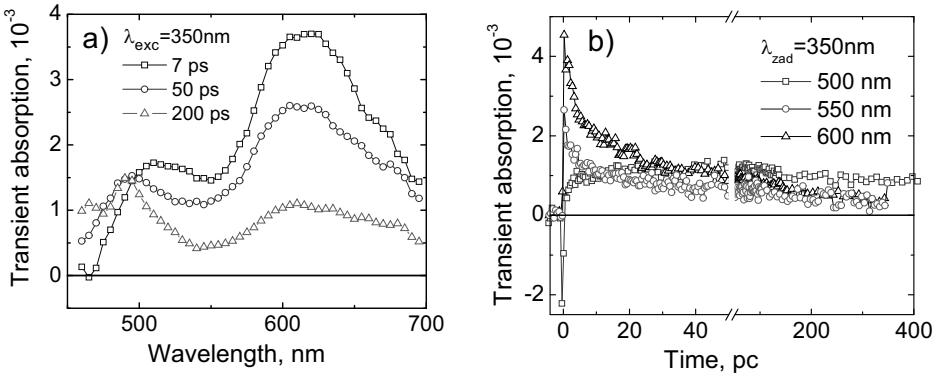

Fig. 6.7. Transient absorption spectra (a) and decay kinetics (b) of G5 PPI dendrimer measured with excitation at 350 nm.

A weak negative signal at 7 ps delay time appears only in the short wavelength side of our accessible spectral range below 470 nm. The transient absorption kinetics presented in both Fig. 6.6 and 6.7 show that the short living stimulated emission is also present at 500 nm, but its decays very rapidly with decay kinetics almost limited by the time resolution of our setup.

Transient absorption at 500 nm (see Fig. 6.8) experiences dramatic changes upon changing the excitation wavelength. The kinetics reveals two transient absorption components: a rapidly relaxing stimulated emission and a slowly relaxing induced absorption. Only the induced absorption is observed under the sample excitation at 330 nm to the long wavelength edge of the enol tautomeric form absorption band. Therefore, we conclude that excited enol

tautomers do not show stimulated emission in the fluorescence band region, but show a short living stimulated emission at shorter wavelength. This is not surprising because enol tautomers have absorption band at about 300 nm and one may expect their fluorescence and stimulated emission band to be located in the UV spectral region. The rapid stimulated emission decay is also in agreement with the excited state dynamics of other molecules experiencing enol-keto tautomerism. As was demonstrated in [190] two competitive processes take place on a fs time scale in the excited enol state of salicylidene aniline: molecule twisting forming twisted-enol state and intramolecular proton transfer forming excited keto state. Thus, the transient absorption band at 630 nm is evidently related to one of these photoproduct states. Moreover, keto tautomers, excited directly and converted from enol tautomers, have different spectral properties [188].

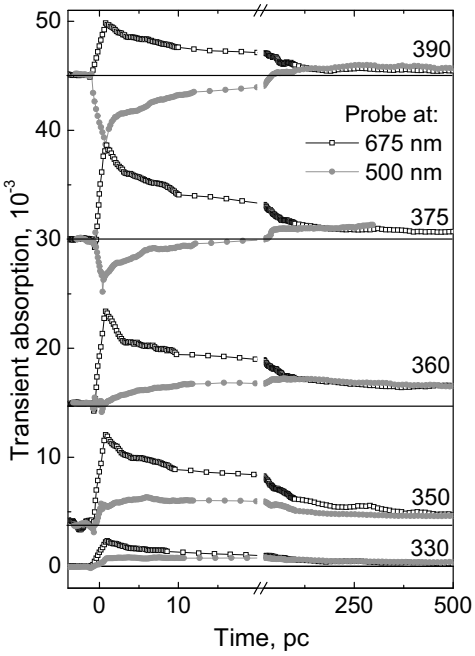

Fig. 6.8, Transient absorption decay kinetics of G5 dendrimer obtained after the different excitation wavelengths and measured at 500 nm and 675 nm.

6.3. Short summary

Bonding of the 4-(4′-ethoxybenzoyloxy)salicylaldehyde chromophore moiety to the amine-terminated PPI dendrimers results in formation of Schiff base containing salicylidenimine functional groups. Steady state absorption spectra and transient absorption investigations of the PPI-ESA dendrimers reveal several tautomeric forms of terminating groups coexisting in dendrimers in

chlorophorm solution. Relative concentrations of different tautomeric forms depend on the dendrimer generation. Based on the analysis of the absorption spectra and quantum chemistry calculation results, we attribute the high intensity absorption band at about 300 nm to enol-closed tautomers, lower intensity absorption band at about 400 nm to *cis*-keto tautomers and the absorption band at about 375 nm observable only in G5 dendrimers to *trans*-keto tautomers. We attribute the dependence of the tautomeric forms on the dendrimer generation to the interaction between dendrimer chains impeding terminating groups to form the lowest energy conformational states.

Transient absorption investigations reveal different absorption properties and relaxation dynamics of different tautomeric forms. Excited *cis*-keto tautomers decay to the weakly fluorescent excited state during about 10 ps and form conformationaly distorted photoproduct states absorbing in the blue spectral region. Excited enol-closed tautomers relax to photoproduct states on a subpicosecond time scale, however they form different photoproducts than excited cis-keto tautomers. Only a small fraction of terminating groups forms fluorescent states, which are identical for all tautomeric forms, however formation yields are different.

Presence of several tautomers with overlapping absorption and excited state absorption spectra impede a more detail determination of the spectral and dynamical properties of different tautomeric forms. Nevertheless, the performed investigations demonstrate a possibility to control tautomeric forms and, thus, the properties of the investigated dendrimers by light.

General conclusions

1. Ultrafast relaxation of PPI and PAMAM dendrimers functionalized with CAzPA type photochromic terminal groups is caused by the excited state *trans-cis* isomerization. In the dendrimer solutions, relaxation occurs on a time scale of several picoseconds and its rate is insensitive to the dendrimer core, solvent and excitation wavelength. The isomerization rate take place within approximately 15 ps in solid dendrimer film, which is seven times slower than in solvents. This indicates, that isomerization rate is determined mainly by the flexibility of the chromophore groups and their interactions with other dendrimer parts as than interaction with the dendrimer environment.

2. Theoretical and experimental investigations of the PPI-ESA dendrimers reveal four most stable tautomeric forms of ESA terminating groups coexisting in dendrimers in chlorophorm solution. Based on the analysis of the absorption spectra and quantum chemistry calculation results, it was shown that domination of the tautomeric forms within the ESA type chromophore groups of PPI dendrimer depends on its generation. Transient absorption investigations have demonstrated that fluorescence yield and excited state dynamics of different tautomeric forms depend on the excitation wavelength. Enol-keto tautomerism and dynamic properties of the ESA type chromophore groups are determined by the hydrogen bonds between chromophore groups.

3. Light induced *trans-cis* isomerization and enol-keto tautomerization of CAzPA and ESA functional groups of dendrimers provides opportunities to control optical and structural changes of dendrimers.

.

References

[1] B. Helms and E.W. Meijer, *Science*, **313**, 929 (2006).

[2] R. Dolencle and A.-M. Caminade, *J. Photochem. Photobiol. C: Photochem. Rev.*, **11**, 25 (2010).

[3] J.-W. Weener and E.W. Meijer, *Adv. Mater.*, **12**, 741 (2000).

[4] N. Malic, J.A. Campbell, A.S. Ali, M. York, A. D'Souza, and R.A. Evans, *Macromolecules*, **43**, 8488 (2010).

[5] V. Shibaev, A. Bobrovsky, and N. Boiko, *Prog. Polym. Sci.*, **28**, 729 (2003).

[6] A. Archut, G.C. Azzellini, V. Balzani, L. De Cola, and F. Vögtle, *J. Am. Chem. Soc.*, **120**, 12187 (1998).

[7] A. Momotake and T. Arai, *Polymer*, **45**, 5369 (2004).

[8] Y. Zeng, Y.-Y. Li, and J. Chen, Guoqiang Yang, Yi Li, *Chemistry An Asian Journal*, **5**, 992 (2010).

[9] R. Mülhaupt, *Macromol. Chem. Phys.*, **211**, 121 (2010).

[10] R. Mülhaupt, *Angew. Chem. Int. Ed.*, **43**, 1054 (2004).

[11] a) P.J. Flory. *J. Am. Chem. Soc.*, **63**, 3083 (1941).; b) P.J. Flory. *J. Am. Chem. Soc.*, **63**, 3091 (1941); c) P.J. Flory. *J. Am. Chem. Soc.*, **63**, 3096 (1941).

[12] E.Buhleier, W.Wehner, and F.Vögtle, *Synthesis*, **155** (1978).

[13] D. A. Tomalia, H. Baker, J. Dewald, M. Hall, G. Kallos, S. Martin, J. Roeck, J. Ryder and P. Smith, *Polym. J.,* **17**, 117 (1985).

[14] D.A. Tomalia, *Aldrichimica Acta*, **37**, 39 (2004).

[15] D. Taton, X. Feng, and Y. Gnanou, *New J. Chem.*, **31**, 1097 (2007).

[16] S.J. Teertstra and M. Gauthier, *Prog. Polym. Sci.*, **29**, 277 (2004).

[17] A.D. Schlüter and J.P. Rabe, *Angew. Chem. Int. Ed.*, **39**, 864 (2000).

[18] K. Inoue, *Prog. Polym. Sci.*, **25**, 453 (2000).

[19] F. Vögtle, G. Richardt, and N. Werner, *Dendrimer Chemistry: Concepts, Synthesis, Properties, Applications,* Wiley-VCH, Weinheim, (2009).

[20] G.R. Newcome, Z. Yao, G.R. Baker, and V.K. Gupta, *The Journal of Organic Chemistry*, **50**, 2003 (1985).

[21] C.J. Hawker and J.M.J. Fréchet, *J. Am. Chem. Soc.*, **113**, 7638 (1990).

[22] F. Zeng and C. Zimmerman, *Chem. Rev.*, **97**, 1681 (1997).

[23] A.W. Bosman, H.M. Janssen, and E.W. Meijer. *Chem. Rew.,* **99,** 1665 (1999).

[24] B. Klajnert and M. Bryszewska, *Acta Biochimica Polonica*, **48**, 199 (2001).

[25] U. Boas, J.B. Christensen, and P.M.H. Heegaard, *Dendrimers in Medicine and Biotechnology: New Molecular Tools*, Royal Society of Chemistry (2006).

[26] J.M.J. Fréchet, *PNAS*, **99**, 4782 (2002).

[27] H. Collet, E. Souaid, H. Cottet, A. Deratani, L. Boiteau, G. Dessalces, J.-C. Rossi, A. Commeyras, and R. Pascal, *Chem. Eur. J.*, **16**, 2309 (2010).

[28] S.A. Ponomarenko, N.I. Boiko and V.P. Shibaev, *Polym. Sci., Ser. C*, **43**, 1 (2001).

[29] J.C. Ribierre, G. Tsiminis, S. Richardson, G.A. Turnbull, and I.D.W. Samuel, *Applied Physics Letters*, **91**, 081108 (2007).

[30] J. Lee, D. Choi, and E.J. Shin, *Spectrochimica Acta Part A*, **77**, 478 (2010).

[31] A. Dirksen and L.D. Cola, *C. R. Chimie*, **6**, 873 (2003).

[32] S. Hecht and J.M.J. Fréchet, *Angew. Chem. Int. Ed*., **40**, 74 (2001).

[33] S.J.E. Mulders, A.J. Brouwer, and R.M.J. Liskamp, *Tetrahedron Lett.*, **38**, 3085 (1997).

[34] R.L. Stears, R.C. Getts, and S.R. Gullans, *Physiol Genomics*, **3**, 93 (2000).

[35] M. Ballauff and C.N. Likos, *Angew. Chem. Int. Ed.*, **43**, 2998 (2004).

[36] P. Marchand, L. Griffe, A.-M. Caminade, J.-P. Majoral, M. Destarac, and F. Leising, *Org. Lett.*, **6**, 1209 (2004).

[37] G.T. Hermanson, *Bioconjugate Techniques*, Elsevier, London, (2008).

[38] D. Astruc, E. Boisselier, and C. Ornelas, *Chem. Rev.*, **110**, 1857 (2010).

[39] U. Gupta, H.B. Agashe, A. Asthana, and N.K. Kain, *Biomacromolecules*, **7**, 649 (2006).

[40] P.G. de Gennes and H. Hervet, *J. Physique – Lettres*, **44**, L-351 (1983).

[41] R.L. Lescanec and M. Muthukumar, *Macromolecules*, **23**, 2280 (1990).

[42] D. Boris and M. Rubinstein, *Macromolecules*, **29**, 7251 (1996).

[43] R. Scherrenberg, B. Coussens, P. van Vliet, G. Edouard, J. Brackman, and E. de Brabander, *Macromolecules*, **31**, 456 (1998).

[44] Y.-J. Sheng, S. Jiang, and H.-K. Tsao, *Macromolecules*, **35**, 7865 (2002).

[45] P.K. Maiti, T. Cahin, G. Wang, and W.A. Goddard, III, *Macromlecules*, **37**, 6238 (2004).

[46] P.K. Maiti, Y. Li, T. Cagin, and W.A. Goddard III, *J. Chem. Phys.*, **130**, 144902 (2009).

[47] A.M. Naylor, W.A.I. Goodard, G.E. Kiefer, D.A. Tomalia, *J. Am. Chem. Soc.*, **111**, 2339 (1989).

[48] K.R. Goppidas, A.R. Leheny, G.Caminati, N.J. Turro, and D.A. Tomalia, *J. Am. Chem. Soc.*, **113**, 7335 (1991).

[49] J.T. Bosko, B.D. Todd, and R.J. Sadus, *J. Chem. Phys.*, **124**, 044910 (2006).

[50] J. Li, L.T. Piehler, D. Qin, R.J. Baker, Jr., D.A. Tomalia, and D.J. Meier, *Langmuir*, **16**, 5613 (2000).

[51] C.L. Kackson, H.D. Chanzy, F.D. Booy, B.J. Drake, D.A. Tomalia, B. Bauer, and E.J. Amis, *Macromolecules*, **31**, 6259 (1998).

[52] J.D. Epperson, L.-J. Ming, B.D. Woosley, G.R. Baker, and G.R. Newkome, *Inorg. Chem.*, **38**, 4498 (1999).

[53] E.J.H. Put, K. Clays, A. Persoons, H.A.M. Biemans, C.P.M. Luijkx, and E.W. Meijer, *Chem. Phys. Lett.*, **260**, 136 (1996).

[54] A. Ramzi, R. Scherrenberg, J. Brackman, J. Joosten, and K. Mortensen, *Macromolecules*, **31**, 1621 (1998).

[55] C. Galliot, C. Larre, A.M. Caminade, and J.P. Majoral, *Science*, **277**, 1981 (1997).

[56] R.M. Crooks, Lemon III, L.Sun, L.K. Yeung, M. Zhao, *Dendrimers-Encapsulated Metals and Semiconductors: Synthesis, Characterization, and Applications*, Springer-Verlag, Berlin-Heidelberg, (2001).

[57] G.R. Newkome, C.N. Moorefield, G.R. Baker, M.J. Saunders, S.H. Grossman, *Angew. Chem. Int. Ed*, **30**, 1178 (1991).

[58] J.F.G.A. Jansen, E.M.M. de Brabander-van den Berg, and E.W. Meijer, *Science*, **266**, 1226 (1994).

[59] F. Aulenta, W. Hayes, and S. Rannard, *Eur. Polym. J.*, **39**, 1741 (2003).

[60] S. Svenson and D.A. Tomalia, *Advanced Drug Delivery Reviews*, **57**, 2106 (2005).

[61] Y. Li, X. Jia, M. Gao, H. He, G. Kuang, and Y. Wei, *J. of Polym. Sci.: Part A*, **48**, 551 (2010)

[62] T.Pradeep and Anshup, *Thin Solid Films*, **517**, 6441 (2009).

[63] Y. Niu and R.M. Crooks, *C. R. Chimie*, **6**, 1049 (2003).

[64] R.W.J. Scott, O.M. Wilson, and R.M. Crooks, *J. Phys. Chem. B*, **109**, 692 (2005).

[65] S.-K. Oh, Y. Niu, and R.M. Crooks, *Langmuir*, **21**, 10209 (2005).

[66] P. Welch and M. Muthukumar, *Macromolecules*, **31**, 5892 (1998).

[67] I. Lee, B.D. Athey, A.W. Wetzel, W. Meixner, and J.R. Baker, Jr, *Macromolecules*, **35**, 4510 (2002).

[68] P.B. Maiti, T.Cagin, S.-T. Lin, and W.A. Goodard, III, Macromolecules, **38**, 979 (2005).

[69] Y. Liu, V.S. Bryantsev, M.S. Diallo, and W.A. Goddard III, *J. Am. Chem. Soc.*, **232**, 2798 (2009).

[70] M. Adeli, Z. Zarnegar, and R. Kabiri, *Journal of Applied Polymer Science*, **115**, 9 (2009).

[71] Y. Bobrovsky, N.I. Boiko, and V.P. Shibaev, *J. Photochem. Photobiol. A: Chemistry*, **138**, 261 (2001).

[72] C. Ornelas, R. Pennell, L.F. Liebes, and M. Weck, *Org. Lett.*, **13**, 976 (2011).

[73] Y. Wang, R. Guo, X. Cao, M. Shen, and X. Shi, *Biomaterials*, **32**, 3322 (2011).

[74] T.H. Ghaddar, J.F. Wishart, D.W. Thompson, J.K. Whitesell, and M.A. Fox, *J. Am. Chem. Soc.*, **124**, 8285 (2002)

[75] F.V.R. Neuwahl, R. Righini, A. Andronov, P.R.L. Malenfant, and J.M.J. Frechet, *J. Phys. Chem. B*, **105**, 1307 (2001).

[76] A. Bobrovsky, S. Ponomarenko, N. Boiko, V. Shibaev, E. Rebrov, A. Muzafarov, and J. Stumpe, *Macromol, Chem. Phys.*, **203**, 1539 (2002).

[77] D.M. Junge and D.V. McGrath, *Chem. Commun*., 5265 (1997).

[78] V. Balzani, P. Ceroni, S. Gestermann, M. Gorka, C. Kauffmann, and F. Vögtle, *Tetrahedron*, **58**, 629 (2002).

[79] M. Longmire, P.L. Choyke, and H. Kobayashi, *Curr. Top. Med. Chem.*, **8**, 1180 (2008).

[80] J. Nithyanadhan, N. Jayaraman, R. Davis, and S. Das, *Chem. Eur. J.*, **10**, 689 (2004).

[81] A. Momotake, M. Uda, and T. Arai, *J. Photochem. Photobiol. A: Chemistry***, 158,** 7 (2003).

[82] R. H. E. Halabieh, O. Mermut, and C. J. Barrett, *Pure Appl. Chem*., **76,** 1445 (2004).

[83] M. Smet, J.-X. Liao, W. Dehaen, and D.V. McGrath, *J. Am. Chem. Soc.*, **2**, 511 (2000).

[84] F. Puntoriero, G. Bergamini, P. Ceroni, V. Balzani, and F. Vögtle, *New J. Chem.*, **32**, 401 (2008).

[85] H. B. Laurent and H. Dürr, *Pure Appl. Chem.*, **73**, 639 (2001).

[86] J.V. Houten, *J. Chem. Ed.*, **79**, 548 (2002).

[87] G.B. Kauffman and L.M. Kauffman, *Chem. Educator*, **7**, 100 (2002).

[88] J.F. Uppenbrink, P. Szuromi, J. Yeston, and R. Coontz, *Science*, **321**, 783 (2008).

[89] J.C. Crano and R.J. Guglielmetti, *Organic and thermochromic compounds*, Springer, New York, (1999).

[90] H. Dürr and H. Bouas Laurent, *Photochromism. Molecules and Systems*, Elsevier, Amsterdam, (2003).

[91] N. Hampp and A. Silber, *Pure & Appl. Chem.*, **68**, 1361 (1996).

[92] B.P. Kietis, P. Saudargas, G. Varo, and L. Valkunas, *Eur. Biophys. J.*, **36**, 199 (2007).

[93] Y. Ohko, T. Tatsuma, T. Fujii, K. Naoi, C. Niwa, Y. Kubota, and A. Fujishima, *Nature Materials*, **2**, 29 (2003).

[94] J. Okumu, C. Dahmen, A.N. Sprafke, M. Luysberg, G. von Plessen, and M. Wuttig, *J. of Appl. Phys.*, **97**, 094305 (2005).

[95] A.I. Gavrilyuk, *Phys. Rev. B*, **75**, 195412 (2007).

[96] H.W. Songand and M. Nogami, *J. Non-Cryst. Solids*, **297**, 113 (2002).

[97] C. Bechinger, E. Wirth, and P. Leiderer, *Appl. Phys. Lett.*, **68**, 2834 (1996).

[98] J. Zmija and M.J. Malachowski, *Archives of Mat. Sci. and Engineer.*, **33**, 101 (2008).

[99] T. He and J. Yao, *Prog. Mater. Sci.*, **51**, 810 (2006).

[100] T. Torster, *Pure. Appl. Chem.*, **24**, 443 (1970).

[101] N.J. Turro, J. McVey, V. Ramamurthy, and P. Lechtnek, *Angew. Chem. Int. Ed.*, **18**, 572 (1979).

[102] A.H. Zewail, *Pure Appl. Chem.*, **72**, 2219 (2000).

[103] R.W. Schoenlein, L.A. Peteau, R.A. Mathies, and C.V. Shank, *Science*, **254**, 412 (1991).

[104] K.C. Hasson, F. Gai, and P.A. Anfinrud, *PNAS*, **93**, 15124 (1996).

[105] N.J. Turro, V. Ramamurthy and C. Scaiano, *Principles of Molecular Photochemistry: an Introduction*, University Science Books, (2009).

[106] N. Tamai and H. Miyasaka, *Chem. Rev.*, **100**, 1875 (2000).

[107] G.S. Hartley, *Nature*, **140**, 281 (1937).

[108] L. Pauling, *The nature of the chemical bond and the structure of molecules and crystals: an introduction to modern structural chemistry*, Cornell University Press., (1960).

[109] J. Henzl, M. Mehlhorn, H. Gawronski, K.-H. Rieder, K. Morgenstern, *Angew. Chem. Int. Ed.*, **45**, 603 (2006).

[110] E. W.G. Diau, *J. Phys. Chem. A*, **108**, 950 (2004).

[111] F. Vögtle, M. Gorka, R. Hesse, P. Ceroni, M. Maestri, and V. Balzani, *Photochem. Photobiol. Sci.*, **1**, 45 (2002).

[112] B.Y. Choi, S.J. Kahng, S. Kim, H. Kim, H. W. Kim, Y.J. Song, J. Ihm, Y. Kuk, *Phys. Rev. Lett.*, **96**, 156106 (2006).

[113] M. Alemani, M. V. Peters, S. Hecht, K. H. Rieder, F. Moresco, and L. Grill, *J. Am. Chem. Soc.*, **128**, 14446 (2006).

[114] I. K. Lednev, T. Q. Ye, P. Matousek, M. Towrie, P. Foggi, F. V. R. Neuwahl, S. Umapathy, R. E. Hester, and J. N. Moore, *Chem. Phys. Lett.*, **290**, 68 (1998).

[115] L. Óvária, J. Schwarz, M.V. Peters, S. Hecht, M. Wolf, and P. Tegeder, *Int. J. Mass. Spectr.*, **277**, 223 (2008).

[116] H. Rau, *Photochemistry and photophysics*, CRC Press, Boca Raton, (1990).

[117] M. Löweneck, A.G. Milbradt, C. Root, H. Satzger, W. Zinth, L. Moroder, and C. Renner, *Biophysical Journal*, **90**, 2099 (2006).

[118] H. Rau and E. Ludeecke, *J. Am. Chem. Soc.*, **104**, 1617 (1982).

[119] S.G. Mayer, C.L. Thomsen, M.P. Philpott, and P.J. Reid, *Chem. Phys. Lett.*, **314**, 246 (1999).

[120] V. Gulbinas, *Šviesos sukelti molekuliniai vyksmai ir jų lazerinė spektroskopija***,** TEV, 2008, Vilnius.

[121] M. Shimomura and T. Kunitake, *J. Am. Chem. Soc.*, **109**, 5175 (1987).

[122] C.L. Forber, E.C. Kelusky, N.J. Bunce, and M.C. Zerner, *J. Am. Chem. Soc.*, **107**, 5884 (1985).

[123] W.S. Struve, *Chem. Phys. Lett.*, **46**, 15 (1977).

[124] C.G. Morgante and W.S. Struve, *Chem. Phys. Lett.*, **68**, 267 (1979).

[125] T. Fujino, S. Y. Arzhantsev, and T. Tahara, *J. Phys. Chem. A***, 105***,* 8123 (2001).

[126] H. Satzger, S. Sporlein, C. Root, J. Wachtveitl, W. Zinth, and P. Gilch, *Chem. Phys. Lett*., **372**, 216 (2003).

[127] E.R. Talaty and J.C. Fargo, *Chem. Commun.*, **2**, 65 (1967).

[128] P. Sierocki, H. Maas, P. Dragut, G. Richardt, F. Vögtle, L. De Cola, F.A.M. Brouwer, and J.I. Zink, *J. Phys. Chem. B*., **110**, 24390 (2006).

[129] Y. Shirota, K. Moriwaki, S. Yoshikawa, T. Ujike, and H. Nakano, *J. Mater. Chem.*, **8**, 2579 (1998).

[130] J. Shao, Y. Lei, Z. Wen, Y. Dou, and Z. Wang, *J. Chem. Phys.*, **129**, 164111 (2008).

[131] I.K. Lednev, T.Q. Ye, R.E. Hester, and J.N. Moore, *J. Phys. Chem.*, **100,** 13338 (1996).

[132] B. Schmidt, C. Sobotta, S. Malkmus, S. Laimgruber, M. Braun, W. Zinth, and P. Gilch, *J. Phys. Chem. A*., **108***,* 4399 (2004).

[133] H. Schiff, *Annalen*, **131**, 118 (1864).

[134] T.T. Tidwell, *Angew. Chem. Int. Ed.*, **47**, 1016 (2008).

[135] M**.** Ziolek, J. Kubicki, A. Maciejewski, R. Naskrecki, and A. Grabowska, *Chem. Phys. Lett*., **369***,* 80 (2003).

[136] J.M. Ortiz-Sanchez, R. Galabert, M. Moreno, and J.M. Lluch, *J. Chem. Phys*., **129**, 214308 (2008).

[137] H. Kuhn and C. Kuhn, *Chem. Phys. Lett.*, **253**, 61 (1996).

[138] S. Mitra and N. Tamai, *Chem. Phys. Lett*., **282**, 391 (1998).

[139] W.R. Cordoba, J.S. Zugazagoitia, E.C. Fregoso, and J. Peon, *J. Phys. Chem. A*, **111**, 6241 (2007).

[140] [J.M.O. Sanchez, R. Gelabert, M. Moreno, and J.M. Lluch, *J. Chem. Phys.*, **129**, 214308 (2008).

[141] M.Z. Zgierski and A. Grabowska, *J. Chem. Phys*., **112**, 6329 (2000).

[142] S. Park, S. Kim, J. Seo, and S.Y. Park, *Macromolecular Research*, **16**, 385 (2008).

[143] F.V.R. Neuwahl, P. Foggi, and R.G. Brown, *Chem. Phys. Lett.*, **319**, 157 (2000).

[144] S.H. Medina and M.E.H. El-Sayed, *Chem. Rev.*, **109**, 3141 (2009).

[145] S. Hartwig, M.M. Nguyen, and S. Hecht, *Polymer. Chem*., **1**, 69 (2010).

[146] F. Vögtle, H. Fakhrnabavi, O. Lukin, S. Müller, J. Friedhofen and C.A. Schalley, *Eur. J. Org. Chem.*, 4717 (2004).

[147] C. Wörner and R. Mühlhaupt, *Angew. Chem.*, **105**, 1367 (1993).

[148] E.M.M. De Brabander-van den Berg and E.W. Meijer, *Angew. Chem*., **105**, 1370 (1993).

[149] J.M. Fréchet and D.A. Tomalia, *Dendrimers and Other Dendrtic Poymers*, Wiley, NY, (2001).

[150] R.M. Crooks, B.I. Lemon III, L. Sun, L.K. Yeoung, and M. Zhao, *Top. Curr. Chem.*, **212**, 81 (2001).

[151] L. Pastor, J. Barbera, M. Mckenna, M. Marcos, R. Martin-Rapun, J.L. Serrano, G.R. Luckhurst, and A. Mainal, *Macromolecules*, **57**, 9386 (2004).

[152] J. Barbera, M. Marcos, and J.L. Serrano, *Chem. Eur. J.*, **5**, 1834 (1999).

[153] M. Marcos, R. Alcalá, J. Barberá, P. Romero, C. Sánchez, and J.L. Serrano, *Chem. Mater.*, **20**, 5209 (2008).

[154] G. Binnig, C. F. Quate, and Ch. Gerber, *Phys. Rev. Lett.*, **56,** 930 (1986).

[155] A. Alessandrini and P. Facci, *Meas., Sci., Technol.*, **16**, R65 (2005).

[156] M.C. Petty, *Molecular Electronics From Principles to Practice*, Wiley, England (2007).

[157] A. Andronov and J. M. J. Fréchet, *Chem. Commun.*, 1701 (2000).

[158] P.L. Burn, S.-C. Lo, and I. D. W. Samuel, *Adv. Mater.,* **19**, 1675 (2007).

[159] M.O. Gallyamov, R.A. Vinokur, L.N. Nikitin, E.E.S. Galiyev, A.R. Khokhlov, I.V. Yaminsky, and K. Schaumburg, *Langmuir*, **18**, 6928 (2002).

[160] J. Katainen, M. Paajanen, E. Ahtola, V. Pore, and J. Lahtinen, *J.Colloid. Interface Sci*., **304**, 524 (2006).

[161] P.M. Buschbaum, J.S. Gutmann, M. Wolkenhauer, J. Kraus, M. Stamm, D. Smilgies, and W. Petry, *Macromolecules*, **34**, 1369 (2001).

[162] C.S. Kim, S. Lee, E.D. Gomez, J.E. Anthony, and Y.L. Loo, *Appl. Phys. Lett.*, **93**, 103302 (2008).

[163] M.J. Jasmine, M. Kavitha, and E. Prasad, *J. Lumin.*, **129**, 506 (2009).

[164] H.A. Essawy and Herba A. Mohamed, *Journal of Applied Polymer Science*, **119**, 760 (2010).

[165] I.B. Rietveld and D. Bedeaux, *J.Colloid.Interface Sci*., **235**, 89 (2001).

[166] J. Gregorowicz and M. Luszczyk, *Macromolecules*, **40**, 5966 (2007).

[167] C. F. Bohren, D. Huffman, *Absorption and scattering of light by small particles*, John Wiley, New York, (1983)

[168] R. Scherrenberg, B. Coussens, P. van Vliet, G. Edouard, J. Brackman, and E. De Brabander, *Macromolecules*, **31**, 456 (1998).

[169] P. Laven. MiePlot A. software, available at www.philiplaven.com/MiePlot.htm.

[170] M.F. Budyka, O.D. Laukhina, and T.N. Gavrishova, *Russ. Chem. Bull.*, **48**, 1491 (1999).

[171] Zouheir Sekkat and Wolfgang Knoll, *Photoreactive Organic Thin Films*, Elsevier Science, USA, (2002).

[172] P. Smitha, S.K. Asha, *J. Phys. Chem. B*, **111**, 6364 (2007).

[173] H.S. Nalwa, *Polymeric Nanostructures and their Applications,* American Scientific Publishers, Los Angeles, (2006).

[174] V. Gulbinas et al., *J. Phys. Chem. A*, **103**, 3969 (1999).

[175] S.C.J. Meskers, M. Bender, J. Hübner, Yu.V. Ramanovskii, M. Oestreich, A.P.H.J. Schenning, E.W. Meijer, and H. Bässler, *J. Phys. Chem. A*, **105**, 10220 (2001).

[176] B. Mollay, U. Lemmer, R. Kersting, R.F. Mahrt, H. Kurz, H.F. Kauffmann, and H. Bassler, *Phys. Rev. B*, **50**, 10769 (1994).

[177] M. Scheidler, U. Lemmer, R. Kersting, S. Karg, W. Riess, B. Cleve, R.F. Mahrt, H. Kurz, H. Bässler, E.O. Göbel, P. Thomas, *Phys. Rev. B*, **54**, 5536 (1996).

[178] R. Kersting, U. Lemmer, M. Deussen, H.J. Bakker, R.F. Mahrt, H. Kurz, V.I. Arkhipov, H. Bässler, E.O. Göbel, *J. Chem.Phys.*, 106, 2850 (1997).

[179] U. Rauscher, H. Bässler, *Macromolecules*, **23**, 398 (1990).

[180] R. Richert, H. Bässler, *Chem. Phys. Lett.,***118**, 235 (1990).

[181] G.B. Talapatra, D.N. Rao, P.N. Prasad, *J. Phys. Chem*., **88**, 4636 (1984).

[182] W. Schrof, E. Betz, H. Port, H.C. Wolf, *Chem. Phys*., **118**, 4636 (1984).

[183] K.M. Gaab, C.J. Bardeen, *J. Phys. Chem. B*, **108**, 4619 (2004).

[184] V. Gulbinas, I. Minevičiūtė, D. Hertel, R. Wallander, A. Yartsev, and V. Sundström, *J. Chem. Phys.*, **127**, 144907 (2007).

[185] M.M.-L. Grage, P.W. Wood, A. Ruseckas, T. Pullerits, W. Mitchell, P.L. Burn, I.D.W. Samuel, V. Sundström, *J. Chem. Phys*., **118**, 7644 (2003).

[186] F.-Y. Dupradeau, D.A. Case, C. Yu, R. Jimenez, and F.E. Romesberg, *J. Am. Chem. Soc.*, **127**, 15612 (2005).

[187] M. Ziolek, J. Kubicki, A. Maciejewski, R. Naskrecki, W. Luniewski, and A. Grabowska, *J. Photochem. Photobiol. A: Chemistry*, **180**, 101 (2006).

[188] R. Karpicz, V. Gulbinas, A. Lewanowicz, M. Macernis, J. Sulskus, L. Valkunas, *J. Phys. Chem. A*, **115**, 1861 (2011).

[189] H. Joshi, F.S. Kamounah, C. Gooijer, G. van der Zwan, and L.J. Antonov, *J. Photochem. Photobiol. A: Chemistry*, **152**, 183 (2002).

[190] M. Sliwa et al., *Photochem. Photobiol. Sci.*, **9**, 661 (2010).

Reziumė

Dendrimerai tai naujai dendritinių polimerų klasei priskiriamos makromolekulės. Jų dydis, funkcinių grupių skaičius yra tiksliai apibrėžti ir gali būti kontroliuojami sintezės metu. Dėl išskirtinių struktūrinių savybių, dendrimerai jau keletą dešimtmečių yra intensyviai tyrinėjamos medžiagos. Viena iš priežasčių, nulėmusių didelį susidomėjimą šiomis medžiagomis yra susijusi su santykinai nesudėtingu molekulės struktūrinių dalių modifikavimu. Sintezės metu vidinėje dalyje įvedant arba prie išorėje esančių chemiškai aktyvių funkcinių grupių prijungiant tam tikrus cheminius junginius, savo ruožtu galima sukurti naujas medžiagas, kurios pasižymėtų neįprastomis savybėmis. Galiausiai, toks šių molekulių struktūros ir savybių kontroliavimas jau leidžia dendrimerus naudoti daugelyje mokslo ir pramonės sričių.

Dendrimerų funkcionalizavimui tinkamų junginių pasirinkimas yra gausus, todėl dažniausiai priklauso nuo to, kokiems tolimesniems tikslams naujai sukurta medžiaga bus panaudota. Pastaruoju metu daug dėmesio sulaukia įvairios fotochrominės medžiagos, kuriose po sąveikos su šviesa yra iššaukiami molekulių struktūros pokyčiai susiję su juose vykstančiomis fotocheminėmis reakcijomis [3]. Pavyzdžiui, azobenzenas, ar kiti azo-jungtį turintys junginiai, dėl šviesa indukuotos *trans-cis* izomerizacijos, yra taikomi įvairių molekulių struktūros kontroliavimui, tuo pačiu metu pakeisdami ir jų funkcines savybes [4]. Taip pat, esant skirtingoms azo-jungtį turinčių junginių *trans* arba *cis* izomerų optinėms savybėms, šios medžiagos neretai tampa paklausiomis kuriant optinius informacijos saugojimo įrenginius ar kt. [5]. Tuo tarpu fotochrominiai (taip pat ir termochrominiai) junginiai, kuriuose sužadintoje, o taip pat ir pagrindinėje būsenoje vyksta šviesa indukuota vidujmolekulinė ar tarpmolekulinė protono pernaša, susijusi su enol-ketotnine tautomerizacijos reakcija, yra svarbūs norint suprasti daugelį gyvojoje gamtoje vykstančių reiškinių, tokių kaip fotosintezės ar regos mechanizmai.

Siekiant pagerinti ar praplėsti fotochrominių junginių pritaikymo galimybes, o taip pat ir suprasti biologinėse sistemose vykstančius procesus, dauguma jų yra inkorporuojami į įvairias matricas. Ilgą laiką tuo tikslu buvo

naudojami polimerai, o šiuo metu neretai pasitarnauja įvairios biologinės molekulės ar dendrimerai. Kadangi dendrimero makromolekulės struktūra yra tinkama tirti daugelį gyvojoje gamtoje vykstančių procesų, atkartojant didelėse molekulėse: proteinuose, polimeruose ar kitose dugiamolekulinėse terpėse vykstančius procesus, pastaruoju metu jie užima savarbią vietą tarp daugelio fotochrominių junginių tyrimų.

Šio darbo tyrimo objektas yra poli(propileno-imino) (PPI) ir poli(amidoamino) (PAMAM) dendrimerai funkcionalizuoti dviejų tipų fotochrominiais junginiais: cianoazobenzenu (CAzPA) ir 4-(4'-etoksi-benzoil-oksi)salicilo-aldehidu (ESA). Tai medžiagos pasižyminčios šviesa inicijuotomis *trans-cis* izomerizacijos ir enol-keto tautomerizacijos reakcijomis.

Šio darbo tikslas yra ištirti PPI ir PAMAM dendrimerų funkcionalizuotų CAzPA ir ESA funkcinėmis grupėmis optines savybes ir šviesa inicijuotų fotocheminių reakcijų dinamiką, panaudojant kelias tyrimų metodikas. Tokiu būdu buvo siekta nustatyti kaip šių junginių fotocheminių reakcijų dinaminės savybės priklauso nuo dendrimero tipo ir jo dydžio.

Siekiant užsibrėžto tikslo buvo ištirtos PPI ir PAMAM dendrimerų funkcionalizuotų CAzPA junginiais plėvelių ir tirpalų dinaminės savybės. Buvo nustatyta, kad *trans-cis* izomerizacijos sparta nepriklauso nuo dendrimero tipo, tirpiklio ir žadinančios spinduliuotės energijos. Taip pat pastebėta, kad dendrimerų plėvelių sužadintos būsenos relaksacijos trukmė yra apie 15 ps, o tai tik apie 7 kartus lėčiau nei tirpaluose.

Eksperimentiškai ir teoriškai ištyrus skirtingų generacijų PPI dendrimerų funkcionalizuotų ESA fotochrominiais junginiais optinių sužadinimų savybes, buvo nustatytos keturios galimos stabilios ESA funkcinių grupių tautomerinės formos, kurių pagrindinės būsenos energijos yra skirtingos. Siekdami įvertinti tautomerinių formų dominavimą buvo atlikti sužadintos būsenos dinamikos tyrimai parodę, kad ESA funkcių grupių tautomerinių formų dominavimas priklauso nuo dendrimero generacijos.